Review

Junli Wang*, Xiaoli Wang, Jingjing Lei, Mengyuan Ma, Cong Wang, Yanqi Ge and Zhiyi Wei

Recent advances in mode-locked fiber lasers based on two-dimensional materials

https://doi.org/10.1515/nanoph-2020-0149
Received March 12, 2020; accepted May 1, 2020

Abstract: Due to the unique properties of two-dimensional (2D) materials, much attention has been paid to the exploration and application of 2D materials. In this review, we focus on the application of 2D materials in mode-locked fiber lasers. We summarize the synthesis methods for 2D materials, fiber integration with 2D materials and 2D materials based saturable absorbers. We discuss the performance of the diverse mode-locked fiber lasers in the typical operating wavelength such as 1, 1.5, 2 and 3 μm. Finally, a summary and outlook of the further applications of the new materials in mode-locked fiber lasers are presented.

Keywords: fiber laser; mode-locked; saturable absorber; two-dimensional materials.

1 Introduction

Ultrafast lasers have attracted increasingly attention in the laser science and technology fields such as precision machining [1–3] and biomedical treatment [4, 5], owing to their high peak power and ultrashort pulses. Meanwhile, the nanotechnology and materials also have been developed widely, due to the continuous progress of ultrafast lasers. Nanotechnology is a powerful tool to investigate and fabricate many emerging materials such as zero-dimensional quantum dots, one-dimensional nanowires, 2D single-atom and three-dimensional nanoballs materials. Physicochemical properties of the materials depend on their structures. Due to the unique properties [6–9], 2D materials have been widely studied and anticipated to have more influence on a diversity of applications. Up to now, the 2D materials family have carbon material [10–12], graphene [13–16], transition metal dichalcogenides (TMD) [17–19], topological insulators (TIs) [20–23], black phosphorus (BP) [24–28], MXenes, etc. [29–32]. In recent several decades, the above 2D materials have been utilized as the nonlinear materials to generate Q-switched and mode-locked lasers. The fiber lasers have many advantages over the other lasers especially the all solid-state lasers due to their compact, high efficiency, robust, free maintenance and low cost [33–36]. Figure 1 shows (a) the evolution of optical systems and (b) evolution of nonlinear optical devices, whose sizes are both reduced dramatically from meters to millimeters and even nanometers. There are plenty of researches on new 2D materials for the generation of mode-locked fiber lasers [37–45], sensors [46], optical switchers and modulators [47–50], optoelectrical devices [51–55] and biomedicine [56–60]. In this work, we review the emerging low dimensional materials and their application of the nonlinear optical properties in the mode-locked fiber lasers. The synthesis methods for 2D materials, fiber integration with 2D materials, especially 2D materials based saturable absorbers (SAs) are summarized. In addition, we discuss and compare the performances of diverse mode-locked fiber lasers in typical operating wavelength such as 1, 1.5, 2 μm and beyond 2 μm. In summary, the outlook and suggestions about the applications of the new materials in mode-locked fiber lasers are given.

***Corresponding author: Junli Wang**, School of Physics and Optoelectronics Engineering, Xidian University, Xi'an, 710071, PR China, E-mail: dispersion@126.com. https://orcid.org/0000-0003-1718-5024
Xiaoli Wang, Jingjing Lei and Mengyuan Ma: School of Physics and Optoelectronics Engineering, Xidian University, Xi'an, 710071, PR China, E-mail: 1523824432@qq.com (X. Wang), 1612486579@qq.com (J. Lei), dkxd05011@163.com (M. Ma)
Cong Wang and Yanqi Ge: Institute of Microscale Optoelectronics, Collaborative Innovation Centre for Optoelectronic Science & Technology, International Collaborative Laboratory of 2D Materials for Optoelectronics Science and Technology of Ministry of Education, Key Laboratory of Optoelectronic Devices and Systems of Ministry of Education and Guangdong Province, College of Physics and Optoelectronic Engineering, Shenzhen Key Laboratory of Micro-Nano Photonic Information Technology, Guangdong Laboratory of Artificial Intelligence and Digital Economy (SZ), Shenzhen University, Shenzhen, 518060, PR China, E-mail: gxgcwang@163.com (C. Wang), geyanqi@hotmail.com (Y. Ge)
Zhiyi Wei: Institute of Physics, Chinese Academy of Sciences, Beijing, 100190, PR China, E-mail: zywei@iphy.ac.cn

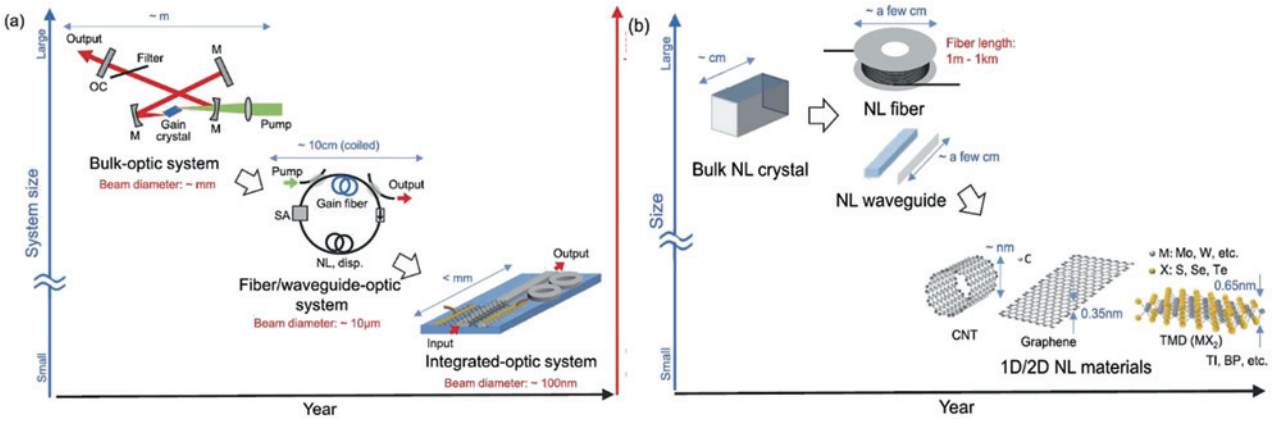

Figure 1: (a) Evolution of optical systems and (b) nonlinear optical devices. Reprinted from ref. [63].

2 Structures and properties of 2D materials

Unlike in bulk materials, the electrons in 2D materials can only move freely in two dimensions, resulting in excellent characteristics such as electron transmission performance, optical and thermal properties. In 2014, Novoselov et al. first exfoliated high-quality single-atom-thick graphene from graphite [61]. After that, a number of novel 2D materials, such as BP, TMD, TIs, MXenes and single-walled carbon nanotube (SWCNT) [62], have been continuously explored. These 2D materials exhibit excellent optical and electrical properties, due to the controlled atomic layer thickness and band gap structure. Therefore, in this section, we focus on the structures and properties of 2D materials.

2.1 Graphene

As we all known, graphene is a single-atom-thick graphite, in which sp^2 hybridized carbon atoms form a planar hexatomic ring structure. The spacing between two adjacent carbon atoms is about 1.42Å [64]. The absorption capability of the almost completely transparent graphene is about 2.3% of the incident light in the infrared visible spectrum [65]. Graphene has excellent optoelectronic and optical properties, such as superior thermal conductivity and high charge carrier mobility. In addition, graphene exhibits good nonlinear optical properties, such as saturable absorption [66], Kerr effect [67], multi-wave mixing [68] and so on. Graphene, a typical semiconductor with a zero-bandgap structure, shows obvious saturable absorption properties when irradiated by high-intensity light. However, the low modulation depth of graphene due to weak absorption characteristics limits its applications in specific wavelength and makes it difficult to achieve ultrashort pulses. Although a higher modulation depth can be obtained by increasing the number of graphene layers, it also increases additional non-saturation loss.

2.2 TMD

TMD are another kind of novel 2D materials with the chemical formula of MX_2, where typically M represents transition metal atom (Mo, W, Re, Ni, Nb, etc.) and X is a chalcogen element (S, Se or Te). Monolayer MX_2 consists of one M layer sandwiched by two X layers. The atoms in the plane are linked by chemical bonds, while the layers are stacked on each other through weak van der Waals forces [69] as depicted in Figure 2 (a). Figure 2(b) and (c) show the atomic force microscope (AFM) image and Raman spectrum of monolayer MoS_2, respectively [70]. In general, the TMD band structure can be gradually transformed from indirect to direct bandgap (1–2 eV), as the layer thickness decreases from multilayers to a single monolayer [71]. It is this unique structure that lead to a wide range of optical, electrical and thermal properties of TMD [72, 73], which are used in transistors, gas sensing, photocatalytic, photodetecting and other fileds [74–77].

2.3 BP

Similar to graphene, a BP monolayer is consisting of a puckered honeycomb structure, in which a single phosphorus atom is connected to three adjacent phosphorus atoms through a covalent bond, and the individual molecule layers interact through weak van der Waals forces (shown in Figure 1(d)). Figure 2(e) and (f) give the high resolution transmission electron microscopy (HR-TEM) image and

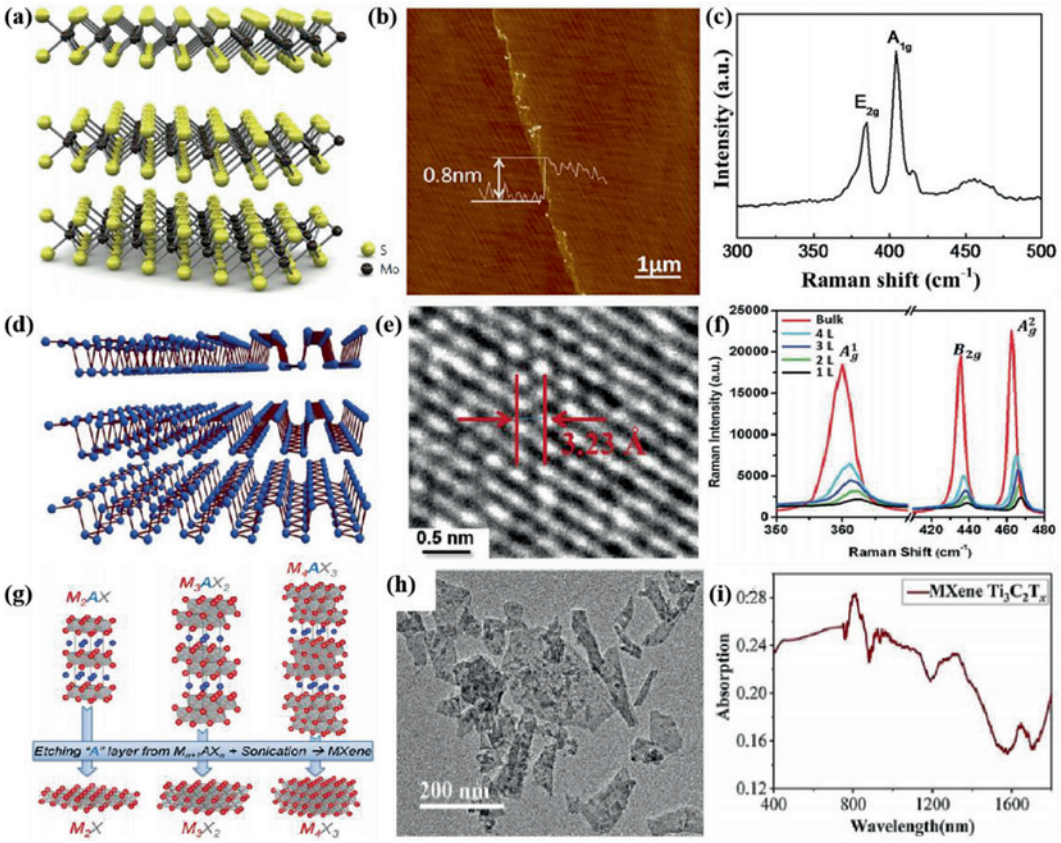

Figure 2: Structure and characteristics of TMD, BP and MXenes. (a) The schematic structure of TMDs, (b) AFM image of MoS_2, and (c) Raman spectrum of monolayer MoS_2. (d) 2D view of the layered BP structure, (e) HR-TEM images of phosphorene and (f) Raman spectras of BP with different numbers of layers. (g) The schematic structure of MAX phase and the corresponding Mxenes, (h) TEM image with scale of 200 nm and (i) The linear absorption spectral of Ti_3CT_2. (a) [69], (b, c) [70], (d–f) [78], (g) [87], (h, i) [88].

layer-dependent Raman spectra of BP [78]. BP has a tunable direct bandgap from 0.3 eV (bulk structure) to 1.5 eV (single layer), connecting the band gap between graphene (zero bandgap) and TMD. Importantly, with increasing layers number, the bandgap decrease [79]. Also, with regard to the BP bandgap, the corresponding wavelength is between 0.6 and 4.0 μm, covering the visible band to infrared region. BP has been widely used in the field of field-effect transistors, photodetectors and solar cells due to the anisotropic in-plane optical, electrical and thermal properties caused by the BP puckered structure [80–82]. However, it is worth noting that BP is highly unstable in the air, which is a quite critical issue and challenge for practical applications.

2.4 TIs

TIs are a class of materials with topological electronic properties. Typical TIs include bismuth telluride (Bi_2Te_3), bismuth selenide (Bi_2Se_3), antimony telluride (Sb_2Te_3), etc. [83]. This type of material has an insulating body state, but the material exhibits metallic properties on the surface due to the existence of a zero-gap Dirac-like electronic bandgap (0.2–0.3 eV) similar to graphene [84]. TIs have an ultra-wide saturation absorption band, extending from visible light to the mid-infrared band. TIs can be used for generating ultrashort pulse lasers due to its narrow band gap and high modulation depth [85]. However, its electron relaxation time is relatively long, which indicates that it is a slow saturable absorber material comparing with graphene [86].

2.5 MXenes

MXenes are a class of 2D transition metal carbides, nitrides or carbonitrides with a general formula of $M_{n+1}AX_n$ (n = 1,2 or 3), where typically M represents transition metal atom (Sc, Ti, Cr, V, Nb, Hf, Ta, etc.), X is carbide and/or nitride and T stands for surface termination unit (O, F, OH, etc.) as shown in Figure 2(g) [87]. MXenes are mainly produced by selective acid etching of the raw MAX phase.

The MAX phases are all hexagonally layered with $P6_3/mmc$ symmetry, where the M layers are almost closely

packed, and X atoms fill the octahedral sites. Element A atomic layer is interleaved with $M_{n+1}X_n$ layers [87]. There are many reports on the characteristics of the MXene. For example, Figure 2(h) and (i) show a transmission electron microscopy (TEM) image and the absorption spectrum of $Ti_3C_2T_x$, reported by Wang [88]. Nowadays, MXene has shown huge potential in diverse fields such as electrochemical catalysis, sensors, photoacoustic imaging, ultrafast photonics, etc. [89–92], due to the advantages of flexible and adjustable composition, controllable thickness and optical, electrical, magnetic properties [93]. Meanwhile, the application of MXenes on ultrafast photonics also have been achieved and demonstrated.

In summary, these 2D materials have many practical applications in sensing, defense, military, biomedical, industrial processing, and other filed due to their unique layered structure and electrical, optical characteristics. However, with the continuous discoveries and researches of 2D materials, the saturable absorption characteristics and pulse shaping mechanism of 2D materials have also been continuously confirmed. Therefore, the ultrafast pulse laser technology based on these 2D materials has attracted much attention both in fundamental researches and in practical applications.

3 Synthesis methods for 2D materials

As shown in Figure 3 [94], the synthesis methods of 2D materials can generally be divided into two types: the top down stripping method and the bottom up growth method.

The top down stripping methods include mechanical exfoliation (ME), liquid phase exfoliation (LPE), chemical exfoliation and laser thinning, which strips bulk materials into mono- or few-layer 2D nanosheets by breaking the van der Waals force between layers [95]. Bottom-up methods, such as chemical vapor deposition (CVD), can directly produce high-quality thin-film materials on molecular level by precisely controlling the chemical reactions between solid precursors. Here, we will briefly introduce three of the material preparation methods that are widely used in mode-locked fiber lasers, including LPE, CVD, and ME.

3.1 ME

The ME technique is widely adopted in the fabrication of atomically and few layers thick sheets of 2D layered inorganic materials [96–99]. By overcoming the van der Waals force and breaking apart layers from bulk materials, researchers can obtain high quality 2D mono- and few-layer materials. Because of its simplicity and ability to produce high-quality few-layer materials, this technique was firstly utilized in discovering graphene from graphite flakes by Geim and Novoselov in 2004 [100, 101]. The exfoliated mono- or few-layer materials have high completeness and less defects, which are suitable for fundamental scientific research. However, the monolayer yield of this process is extremely low; hence, this method is only suitable for laboratory scale studies and cannot be utilized for large-scale production for high-end technological application.

ME using scotch-tape has been reported in many studies for the synthesis of other 2D materials. Monolayer BP is often obtained by this method. In order to minimize the material's exposure to the ambient, Zenghui Wang et al. [102] incorporate special steps uniquely developed to facilitate the transfer of BP after exfoliation. As shown in Figure 4, they carefully stamped a small rectangular piece of polydimethylsiloxane (PDMS) film, whose protection layers were peeled off on both sides, onto a clean glass slide. The BP samples were then exfoliated for dozens of times before transferred onto the PDMS stamp quickly. BP flakes were carefully inspected under optical microscope to identify promising candidates for device fabrication, and stored in vacuum chamber immediately afterward for further investigation.

Although this process is relatively simple, fast and cost effective, it has certain disadvantages. The monolayer obtained by this process is extremely low and repeated operation is required. Hence, this method is only suitable for laboratory scale studies and cannot be utilized for large-scale production for high technological applications.

3.2 LPE

As discussed in the previous section, ME of 2D layered materials suffers from a low production rate that is not technologically scalable in its current form. As an alternative method, LPE is a reliable way to produce single and few layers 2D sheets at bulk scale. LPE can be broadly classified into the following basic categories: (i) oxidation followed by subsequent dispersion into suitable solvents, (ii) ion intercalation, (iii) ion exchange and (iv) ultrasonic exfoliation [103].

Among them, (i–iii) are chemical exfoliation methods which can afford high-yield production of 2D material nanosheets. However, the produced nanomaterials usually has poor dispersion ability. Another prevalent

Figure 3: Classification of fabrication methods of 2D materials. Reprinted from ref. [94].

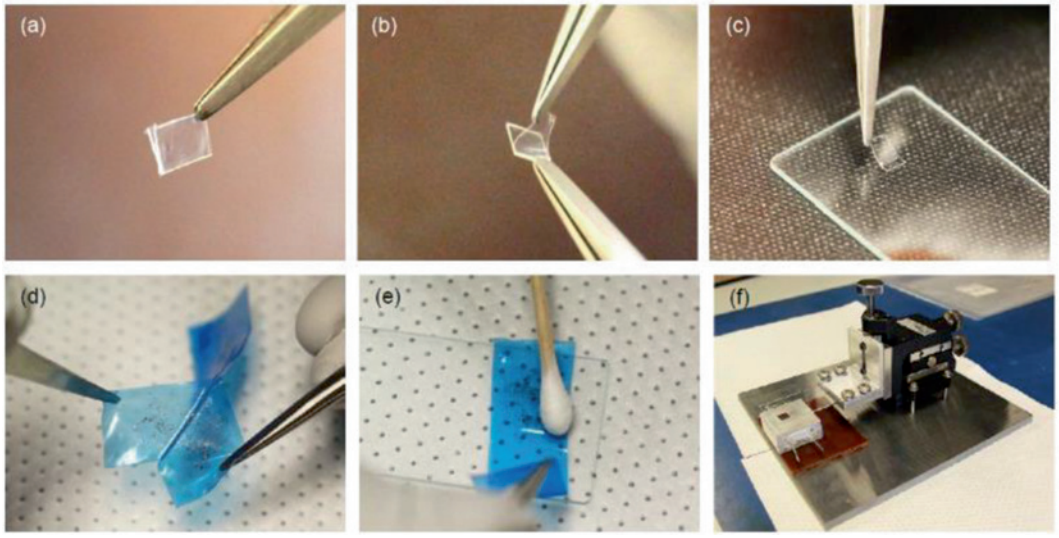

Figure 4: Steps involved in the flake preparation and transfer process. Reproduced with permission [102].

method is ultrasonic exfoliation, which is a purely physical method. This method is to conduct ultrasonic treatment on the material under the action of dispersant, separate the material sheet layer, and obtain the solution of single or few layers after repeated ultrasonic treatment and centrifuge. Figure 5 is an experimental flowchart of the exfoliation process.

3.3 CVD

Generally, 2D materials could be prepared via ME, LPE and CVD. However, few layer materials obtained with the LPE or ME methods usually suffer from uncontrollable size and random thickness [105, 106], which are detrimental for the performance of a SA. As for bottom-up methods, CVD is an important and scalable method to synthesize large-scale 2D materials. The first report on CVD growth of uniform, large area graphene on a metal surface was in 2009. They grew centimeter-sized graphene films on copper substrates by CVD using methane [107]. W. Liu et al. prepared large area and high lattice quality few-layer WSe_2 by CVD and applied it in mode-locked all-fiber laser, as shown in Figure 6 [108].

Few-layer/multilayer materials can be easily prepared by the CVD method. As for the SAs, the modulation depth

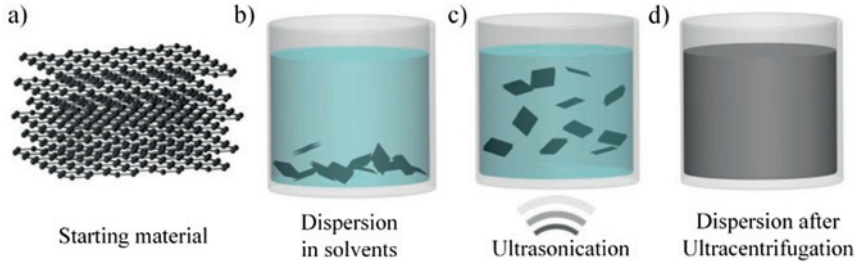

Figure 5: LPE method. (a) Starting material, (b) chemical wet dispersion, (c) ultrasonication and (d) final dispersion after the ultracentrifugation process. Reproduced with permission [104].

can be increased by controlling layer numbers. However, the preparation process is relatively complex and cost is high (e. g., the material films must be carefully transferred onto target substrates, and transfer residues are difficult to remove completely) [108–111].

4 Fiber integration with 2D materials

To fabricate SAs for all-fiber mode-locked ultrafast fiber lasers, many designs have been developed in order to achieve sufficient interaction between 2D materials and intracavity laser light. Generally, these incorporation designs are different for solid-state lasers and fiber lasers. For solid-state lasers, 2D materials are usually plated on high-reflection mirrors to achieve coupling with the beam in free space. For fiber lasers, the coupling should consider the unique fiber property and many special designs have been developed. Figure 7 shows some popular fiber coupling schemes.

In 2007, Yamashita's group first proposed and demonstrates a simple method of sandwich structure, which deposited carbon nanotubes (CNTs) onto the core area of the optical fiber end [112]. The most commonly used is the sandwich structure as shown in Figure 6(a). The prepared 2D materials are embedded in a polymer film, which can be organic polyvinyl alcohol (PVA) [113–118], polymethyl methacrylate (PMMA) [119–123], PDMS [124] and so on. Because the core of a single-mode fiber is usually very small, it is necessary to cut the prepared polymer film into some small individual films and sandwich it between two fiber ferrules for transmission coupling. The main advantage of the sandwiched structure is the strong interaction between the SA and laser signal because of the direct insertion of the SA into the laser cavity, leading to good mode-locking performance [94]. Besides, it has low cost, strong flexibility and strong controllability, which is more conducive to the preparation of SAs. However, the scattering of nanomaterials leads to additional thermal dissipation [108, 125].

To scale the damage threshold of fiber SAs, another common method is to deposit SA materials on a side polished fiber (SPF, also called D-shaped fiber) or tapered fiber to obtain mode-locked lasers. In 2017, Yamashita's group presented fiber integration with CNTs based on SPF and tapered fiber structure for the first time [126, 127]. In this case, the evanescent field of the light beam in the fiber interacts with 2D materials on the side, which reduces the light intensity in the materials. As shown in Figure 7(b), Li et al. show a graphene-clad microfiber modulator, which was assembled by covering a mechanically exfoliated graphene film on the surface of a microfiber [128]. They fabricated electrically controllable in-line graphene devices by integrating graphene-based field effect transistors on a SPF with ionic liquid as electric gating medium (Figure 7(c) [129, 130]).This method allows a very long

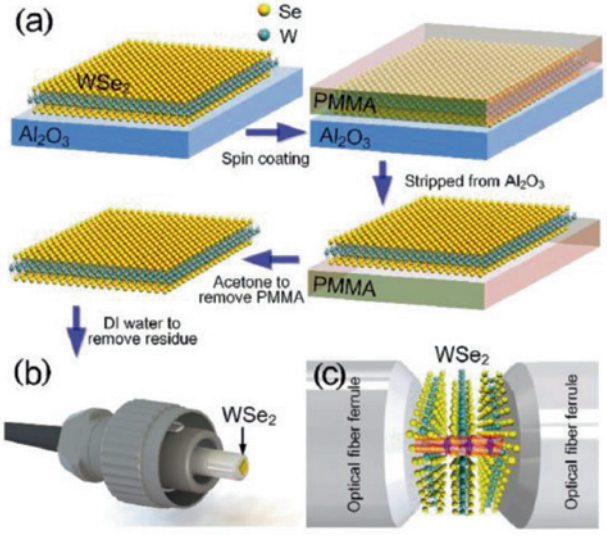

Figure 6: Schematic representation of the preparation of WSe_2-based SA. (a) The transfer process of WSe_2 films. (b) Illustration of WSe_2 films on the end face of the optical fiber ferrule. (c) Illustration of the inter-action between light and few-layer WSe_2. Reproduced with permission [108].

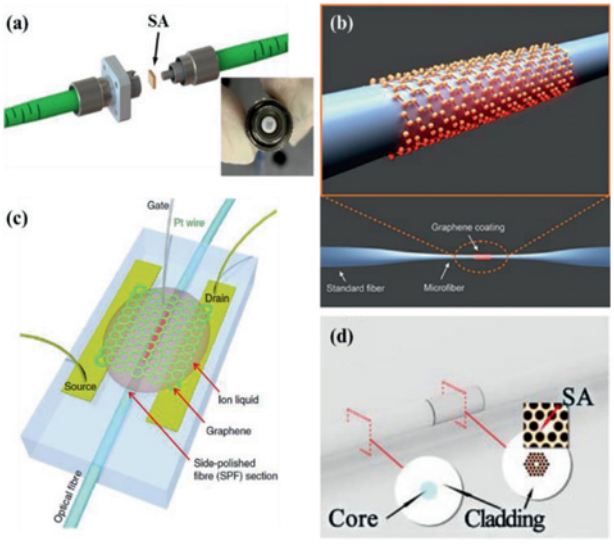

Figure 7: SA incorporation methods: (a) sandwiching SA between two connectors, (b) depositing SAs on tapered fiber, (c) coating SAs on side-polished fiber, and (d) filling SA into hollow photonic crystal fibers (PCFs). (a) [131], (b) [128], (c) [129], (d) [132].

interaction length and therefore is preferred in many experiments investigating optical nonlinearity.

For an alternative approach, Z. B. Liu first reported a fiber laser that was passively mode-locked by filling graphene oxide (GO) solution into the photonic crystal fiber (PCF) as a SA [133]. As shown in Figure 7(d) [132], the prepared material solution can be filled into the PCF with high-pressure injection method. Then, the solution-filled PCF was oven dried in order to remove the solvent and splice with the single-mode fiber [134]. Although PCF-based SA has advantages of stronger interaction effect, longer interaction length and larger nonlinear effect [135], this type of SA device also has some problems such as larger insertion loss, distortion of the guiding mode in the PCF region and so on [136].

5 2D materials as SAs

The Mode-locked fiber lasers are gathering increasing attention from fundamental research to practical applications. The nonlinear saturable absorption properties of low dimension materials play an important part in mode-locked laser mechanism and thus SAs have been utilized to support ultrafast mode-locked operation in the laser cavity. For the mode-locked laser output, the main components of fiber resonant cavity include the pumping source, wavelength division multiplexer (WDM), gain medium (rare earth doped fibers), single mode fiber (SMF), polarization independent/dependent optical isolator (PI-ISO/PD-ISO), polarization controller (PC) and optical coupler (OC). Meanwhile, some important parameters, such as operating wavelength, 3-dB bandwidth, pulse width, repetition rate and single pulse energy, characterize the performance of mode-locked laser. In recent years, a variety of mode-locked fiber lasers working at 1 μm (ytterbium-doped, Yb-doped), 1.5 μm (erbium-doped, Er-doped), 2 μm (thulium-doped, Tm-doped) and ~3 μm (Er-doped ZBLAN) based on novel 2D materials have been widely reported. In the following sections, four typical lasers in different operating wavelengths are summarized and discussed.

5.1 1 μm wavelength mode-locked fiber lasers

Mode-locked fiber lasers working at 1 μm have good application prospects in industrial processing, medical and national defense fields, due to its high efficiency. In general, Yb-doped fibers (YDF) are used as the gain medium in the 1 μm region. Compared with Er-doped fibers (EDF), YDF have a wider gain spectrum, lower quantum loss and higher pumping efficiency, which are conducive to the generation and amplification of high-power lasers. It is universally known that the generation of all-normal dissipative solitons (DS) with bell-shape spectra and large chirp is the result of the balance of gain, loss, spectral filtering, nonlinear effects and dispersion in the laser cavity. In 2012, Li et al. demonstrated a self-started mode-locked YDF laser with GO at different cavity length (Figure 8a–c) [137]. In 2014, Zhang et al. first achieved a stable mode-locking laser with a pulse duration of 800 ps and a single pulse energy of 1.4 nJ based on MoS_2-nanoplantlets SA in the 1 μm region (Figure 8d–f) [138]. Subsequently, all-fiber Yb-doped laser based on various binary materials, such as WS_2, $MoSe_2$, WSe_2, Bi_2S_3, Bi_2Te_3, Sb_2Te_3 and so on, were gradually reported. In addition, some ternary and even multiple materials were discovered for their good nonlinear saturable absorption characteristics and therefore were used as SA to generate laser pulses. In 2019, Ma et al. realized the noise-like mode-locked pulses (NLP) operating at 1 μm wavelength by using few-layer $ReS_{1.02}Se_{0.98}$ nanoflakes as SA (Figure 8g–i) [139]. Here, many typical low dimension materials such as graphene, TMD, TIs and so on, were applied for the ultrashort pulse generation in the 1 μm region and have been presented in Table 1. These corresponding data are also shown in Figure 8, where the vertical axis represents the pulse width and the horizontal axis represents the repetition rate. In Figure 9, the shapes and colors of the marks represent different materials.

In general, YDF lasers were in the all-normal dispersion region where DS were generated. The realization of negative dispersion in YDF lasers cavity was extremely challenging, because there were few anomalous group velocity dispersion (GVD) fibers at 1 μm to compensate for the normal dispersion in the gain fibers and SMF. However, there were some reports that have implemented femtosecond pulses by using dispersion management techniques with grating pairs, PCF, etc. For instance, Z. Zhang et al. directly obtainedan output pulse of 8.7 ps at the exit of the CNT-based YDF cavity. In order to obtain a shorter pulse, a section of 2.1 m-long solid-core PCF was added into the cavity for dispersion management, which allows generation of 118 fs pulse (Ref. [160] in Table 1). Also, Hou et al. designed a dispersion managed YDF laser with a grating pair as compressor, which obtained the shortest pulse width of 175 fs (Ref. [158] in Table 1). To generate ultrashort pulses and large energy output in the cavity is also a common goal pursued by researchers, so Xile Han, et al. demonstrated a mode-locked Yb-doped linear-cavity fiber laser with a total length of 194.54 m, in

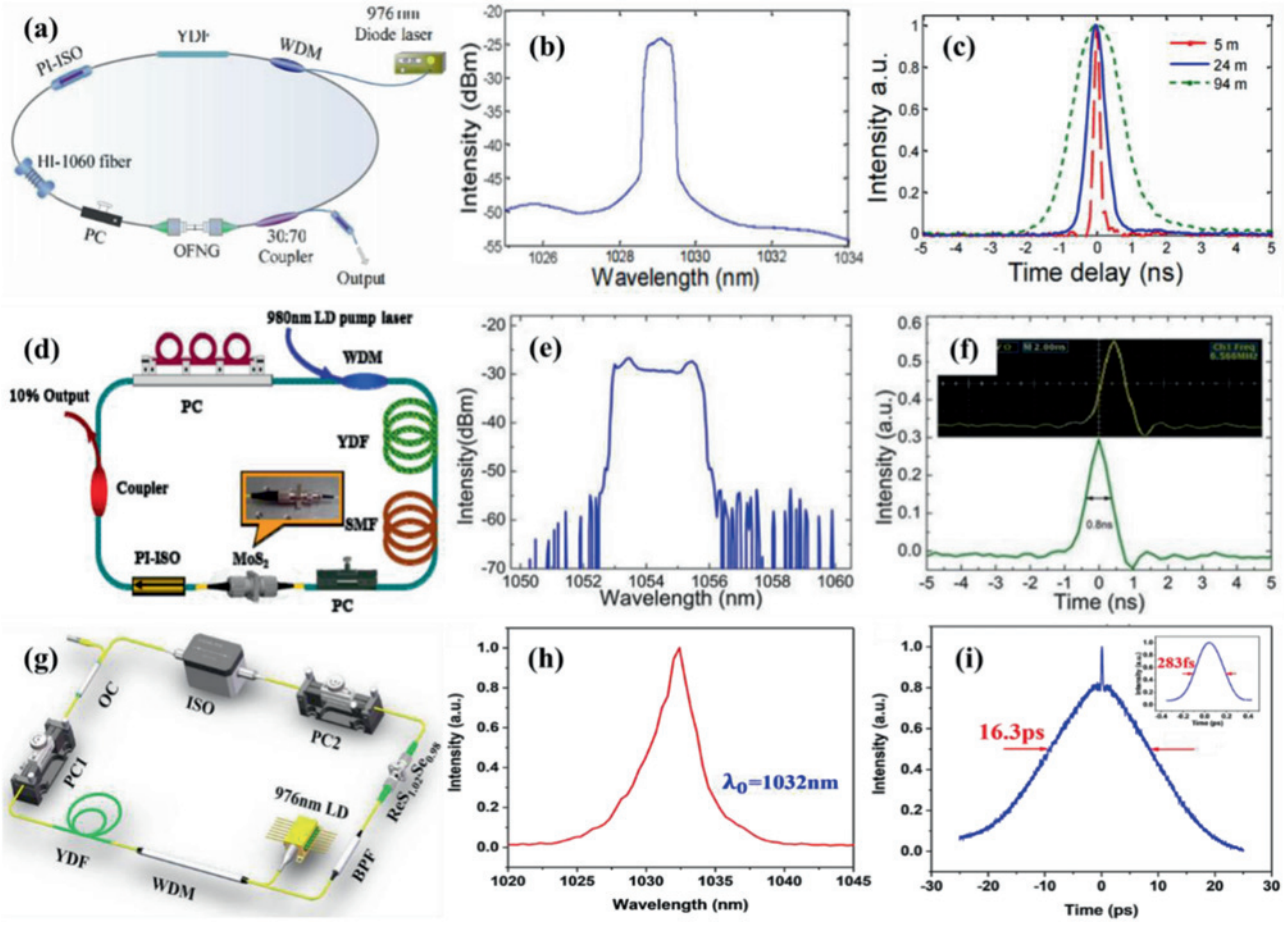

Figure 8: Typical mode-locked fiber lasers working in the 1 μm region. (a) The schematic diagram of the mode-locked YDF laser based on graphene oxide, (b) the optical spectrum with 94 m long cavity and (c) the pulse duration with the different cavity length. (d) Schematic of the YDF laser mode-locked by the MoS_2, (e) the optical spectrum and (f) the oscilloscope tracing. (g) Diagram of the mode-locked fiber setup based on $ReS_{1.02}Se_{0.98}$, (h) optical spectrum and (i) output pulse train (inset: magnified autocorrelation curve of the NLPs). (a–c) [137], (d–f) [138], (g–i) [139].

which the net dispersion in the cavity are 3.45 ps^2. Although the repetition rate in the cavity is relatively low, only 527 kHz, but a higher single pulse energy of 61.8 nJ is obtained (Ref. [184] in Table 1). Furthermore, in 2013, Shasha Li, et al. achieved the output of femtosecond pulses of 93.8 fs with high single pulse energy of 60.1 nJ by using double-clad Yb-doped gain fiber as the gain medium(-Ref. [170] in Table 1).

From Table1 and Figure 9, SWCNT seem to presents the best performance in the generation of shorter pulse output. The output pulse width of YDF lasers based on graphene is relatively wide due to the zero bandgap structure and low modulation depth of the material. Some types of quantum dot (QD) materials such as GaTe QD, $NbSe_2$ QD, PbO QD also are used as SA for mode-locking operation in YDF lasers. Although Sb_2Te_3 obtains the largest bandwidth of 8.87 nm, the mode-locked duration of fiber laser is only 5.9 ps. YDF lasers based on 2D materials basically have a relatively wide output pulse width because it is located in the normal dispersion region and it is not easy to carry out dispersion management due to the lack of anomalous dispersion fibers. However, the DS it generates cause the laser to output high single pulses energy. In addition, perovskites exhibit higher pulse energy than other 2D materials. Therefore, the dispersion management is a critical factor to the output performance in mode-locked fiber lasers.

5.2 1.5 μm wavelength mode-locked fiber lasers

EDF has strong gain at 1.5 μm, and its 40 nm wide spectral profile is the atmospheric window for low loss optical communication. Erbium-doped mode-locked fiber lasers also own high power density, high coupling efficiency, and

Table 1: Performance summary of mode-locked fiber lasers operating at 1 μm by using various 2D materials as SAs.

SA	Repetition rate(MHz)	Output power (mW)	Pulse energy (nJ)	Pulse duration (ps)	3 dB bandwidth (nm)	Center wavelength (nm)	Refs.
Graphene	10.05 (CP)9.55	12.5	1.2	189	1.93	1059.7	[140]
			0.22	2.73	0.75	1057.2	
	1.078	147.5	159.4	0.9 ns	0.19	1064.9	[141]
	1.072	0.19	0.177	2.3 ns	0.477	1064.1	[142]
	14.2	2.1	0.148	147.9	1.95	1059.7	[143]
	0.415	–	–	5.5 ns	0.35	1063.7	[144]
	1.78	3.05	1.713	2.41 ns	4.	1061.8	[145]
	1.78	3.05	1.713	2.2 ns	2.16	1068.8	[145]
	16.29	2.39	0.18	6.5 ns	0.18	1035.1	[146]
	1.04	170	163	680	0.12	1074.7	[147]
	1.05	20	19	520	3	1035	[148]
	10.05	12.5	1.2	202	–	1060	[149]
	0.9	0.37	0.41	560	1.29	1069.8	[150]
	1.062	9.3	8.68	30.9 ns	1.177	1063.3	[151]
BP	16.77	18.9	1.13	51	5.9	1064.4	[152]
	6.78	1.62	0.24	3380	0.17	1063.9	[153]
	18.47	–	–	–	–	1063.8	[154]
	0.38	–	–	39.4 ns	0.1	1067	[155]
Au-nanotube	18.69 (CP)17.94	4.1	–	460	1.2	1068.2	[156]
		0.94	0.053	0.84	1.5	1063.9	
SWCNT	21.5	1.5	0.7	317	0.17	1060.2	[157]
	21.2	8.68	0.41 (CP)0.047	4.14	32.7	1025.5	[158]
				0.175	20.2	1031.5	
	27.2	3.47	0.128	2.43	1.6	1030	[159]
	34	3.5	0.103	8.7/(CP)118 fs	17.6	1037	[160]
	23.4	–	–	0.18	7.5	1032.5	[161]
	21.5	1.5	0.07	317	0.17	1061	[162]
	23.83	92.3	3.87	421.9	0.49	1051.87	[163]
	23	15	0.65	194	2.7	1054.16	[164]
	9.44	1.1	0.116	300	1.82	1036.89	[165]
	41.6	2.1	1.2	380	1.4	1035	[166]
	130	2	0.015	16	0.15	1058.65	[167]
	19.46	2	0.103	276	0.57	1063.3	[168]
	0.199	40.3	201.5	102 ns	0.17	1080.16	[169]
	5.59	336	60.1	0.0938	8.6	1083.8	[170]
	50	155	3	0.235	–	1032	[171]
Bismuthene	21.74	8.36	0.385	30.25	2.72	1034.4	[172]
MoS_2	15.43	1.5	0.097	1550	0.9	1037.5	[173]
	2.025	0.35	0.17	336.5	2.1	1029.3	[174]
	26.5	32	1.21	475	2.6	1037	[70]
	16.51	16.7	1.01	13.7	4.8	979	[70]
WS_2	5.57	76	13.6	630	0.77	1063.6	[175]
	23.26	30	1.29	713	0.29	1052.45	[121]
	–	–	2.82	2400	1	1034.2	[176]
SnS_2	39.33	2.23	0.057	656	8.63	1062.66	[177]
	3.76	0.123	0.033	282	1.2	1031	[178]
	18	1.023	0.057	1050	0.064	1027.71	[179]
Bi_2S_3	3.94	10	2.538	782	0.2	1038	[180]
Bi_2Se_3	44.6	33.7	0.756	46	2.	1031.7	[181]
	1.11	1.2	1.08	960	1.11	1064.47	[135]
Bi_2Se_3	11.38	9.46	0.83	210	1.14	1037.02	[182]
	16	17.1	1.88	380	–	1038.5	[183]
	17.7	1.88	0.1	507	1.4	1039	[183]
	0.527	32.6	61.8	398 ns	–	–	[184]

Table 1: (continued)

SA	Repetition rate(MHz)	Output power (mW)	Pulse energy (nJ)	Pulse duration (ps)	3 dB bandwidth (nm)	Center wavelength (nm)	Refs.
Bi_2Te_3	1.44	0.86	0.599	230	3.69	1057.82	[185]
	19.64	55	2.8	317	1.245	1052.5	[186]
	6.16	12.4	2	5470	2.4	1063.4	[187]
Graphene- Bi_2Te_3	3.77	2.53	–	189.94	3.5	1058.9	[188]
	3.7	–	–	144.3	4.3	1049.1	[189]
Sb_2Te_3	19.38	15.7	0.81	–	2.28	1065.3	[190]
	19.28	4	0.21	5.9	8.87	1047.1	[191]
	19.2	0.57	0.03	5.3	8.82	1036.7	[191]
	17.07	0.54	0.032	0.38	4.25	1039.4	[192]
$PtSe_2$	4.08	12.19	2.31	470	2	1064.47	[193]
	4.45	1.08	0.243	1900	4.7	1067.5	[194]
InSe	1.76	16.3	9.3	1370	1.3	–	[195]
GaTe QD	11.73	9	0.781	752	–	1030.72	[196]
$NbSe_2$ QD	12.3	10.5	0.854	380	0.155	1033	[197]
Mo_2C	3.22	–	–	418	2.62	1061.8	[198]
PbO QD	4.37	24.13	5.52	303	2	1062.12	[199]
$NiPS_3$	8.2	1.66	0.21	126.5	4.86	1066.2	[200]
$CH_3NH_3PbI_3$	4.08	15.71	3.85	913	5.11	1064	[41]
$CH_3NH_3SnI_3$	4.03	28.19	6.99	1770	8.09	1064	[201]
$Ti_3C_2T_x$	18.96	9	0.47	480	4.4	1065.89	[44]
Ti_2CT_x	11.2	–	–	164.4	3.4	1051.08	[202]

CP: after compression.

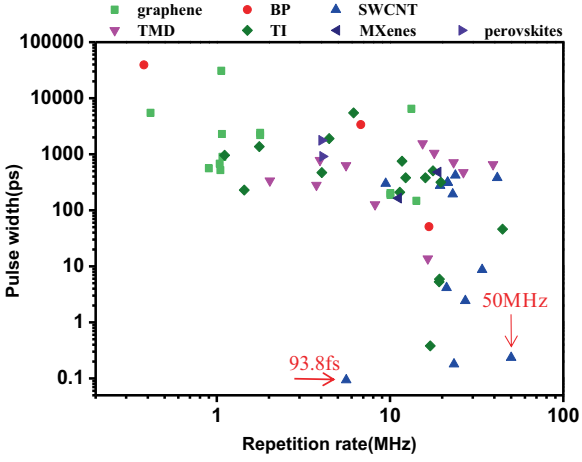

Figure 9: Pulse width versus repetition rate of 2D materials based mode-locked Er-fiber lasers.

compact structure. In 2014, Jeong et al. demonstrated a dissipative soliton fiber laser with high pulse energy based on a SWCNT-SA. The laser stably delivered linearly chirped pulses with a pulse duration of 12.7 ps, and exhibited a spectral bandwidth of 12.1 nm at the central wavelength of 1563 nm. Average power of the laser output was measured as 335 mW (Figure 10(a–c)) [203]. In 2017, Yin et al. studied the saturable absorption of CVD grown WSe_2 films with large-scale and high quality. They used WSe_2 films as a broadband SA for passively mode-locked fiber lasers with the pulse durations of 477 fs at 1.5 μm (Figure 10(d–f)) [204]. In 2018, Liu et al. investigated MoS_2-Sb_2Te_3-MoS_2 heterostructure materials with uniformity by employing the magnetron sputtering technique at 1.5 μm mode-locked fiber laser, which had a large modulation depth and high reliability (Figure 10(g–i)) [205]. Recently, the change in repetition frequency and pulse width of low-dimensional material mode-locked fiber lasers are demomstrated, which is shown in Figure 11.

Unlike YDF lasers, both DS and conventional solitons (CS) can be generated by dispersion management in EDF lasers. Among them, DS will obtain higher single pulse energy, while CS are easier to achieve shorter pulses and slight chirp. Therefore Er-doped lasers can work in both normal and anomalous dispersion regions. For example, Lei Gao, et al. proposed two kinds of (DS and CS) EDF mode-locked laser based on Bi_2Se_3 nanosheets. The CS laser system had a total length of 10.1 m with the net anomalous dispersion of $-0.232ps^2$, which generated 908 fs pulse output. While DS laser obtained a pulse width of 7.564 ps, whose the total length of 29.1 m and the net normal dispersion of $0.104\ ps^2$ (Ref. [229] in Table 2). In addition, there are some reported on the mode-locked due to combined action of a 2D SA and nonlinear polarization evolution (NPE). In 2015, Liu et al. proposed a hybrid mode-locked EDF laser incorporated with Sb_2Te_3, in which NPE was utilized to achieve ultra-short pulses and high average

power output. By this means, the laser system generated ultrashort pulses with the pulse width of 70 fs and average power of 63 mW [262]. Also, Bogusławski et al. demonstrated a hybrid mode-locked fiber laser in the same year, which was observed sub-200 fs pulse output [263].

Compared with the YDF mode-locked lasers, the EDF mode-locked lasers have obvious advantages in generating shorter pulse lasers and more potential applications such as optical communications system, and the frequency comb system. In addition, the smallest transmission loss also exists in the 1.5 μm wavelength in the single mode fiber. In Table 2, the majority of investigations focused on the SWCNT, BP, TIs, and TMD. Few reports revolved in the MXenes and ternary TMD SA, in which TMD SA presents good pulse duration and high repetition rate, as shown in Figure 11. Therefore, TMD is expected to produce better output characteristics in terms of ultrashort pulses and high repetition rates. In addition, the pulse width obtained by the EDF laser based on TIs was less than 5 ps, which also shows an excellent saturable absorption characteristic in the 1.5 μm wavelength. Although the single pulse energy generated by the EDF laser based on 2D materials is relatively small, TIs seem to be more dominant after comparison.

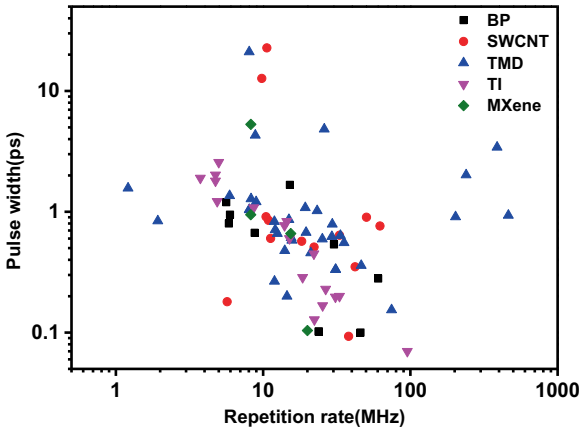

Figure 11: Pulse width versus repetition rate of 2D materials based mode-locked Er-fiber lasers.

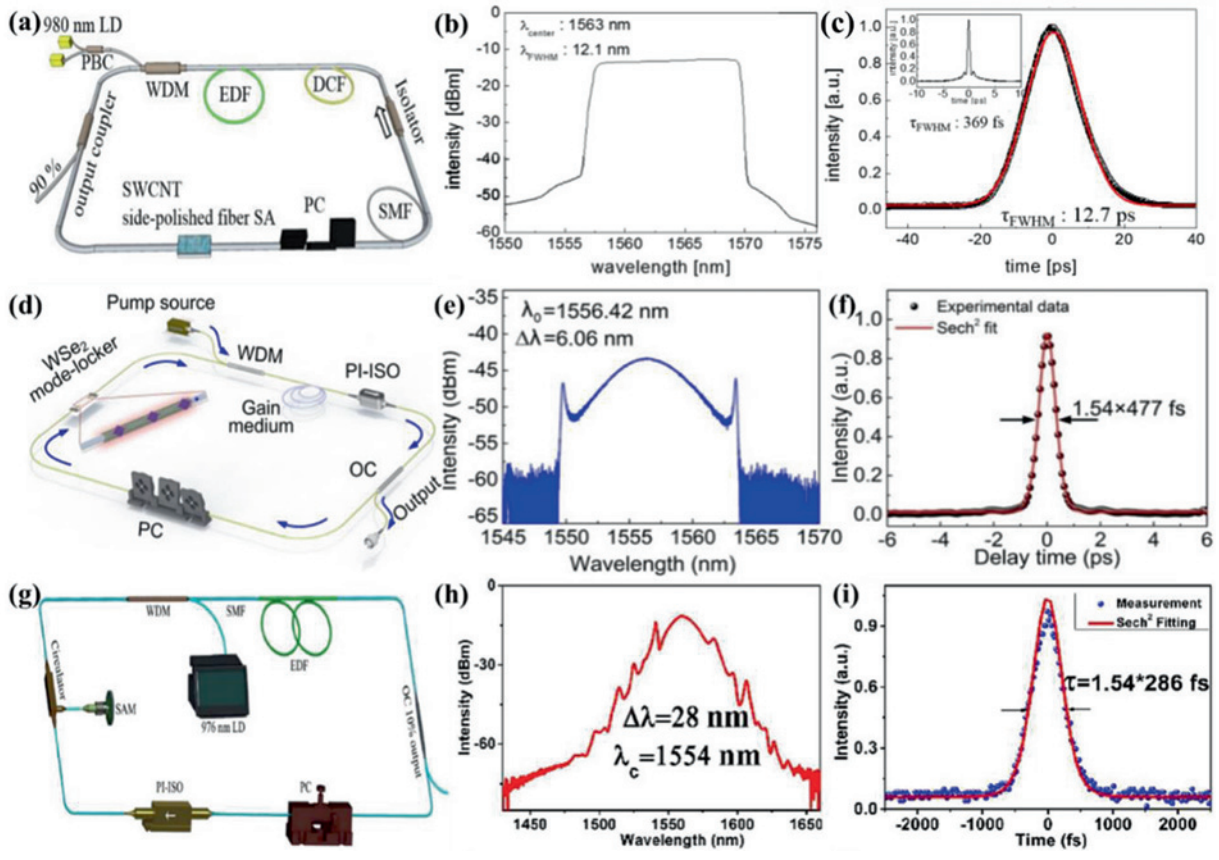

Figure 10: Typical mode-locked fiber lasers working in the 1.5 μm region. (a) configuration of the constructed all-fiber ring laser using an SWCNT-SA, (b) optical spectrum and (c) auto-correlation trace (inset: auto-correlation trace after compression). (d) Schematic illustration of the typical ring cavity of the mode-locked fiber laser based on the microfiber WSe_2 SA, (e) output optical spectrum with solitonic sidebands and (f) auto-correlation trace of mode-locked pulse with a $sech^2$ fitting curve. (g) Configuration of the mode-locked EDF laser based on MoS_2-Sb_2Te_3-MoS_2 heterostructure SA mirror, (h) optical spectrum and (i) pulse duration. (a–c) [203], (d–f) [204], (g–i) [205].

Table 2: Performance summary of mode-locked fiber lasers operating at 1.5 μm by using various 2D materials as SAs.

SA	Repetition rate(MHz)	Output power (mW)	Pulse energy (nJ)	Pulse duration (ps)	3dB bandwidth (nm)	Center wavelength (nm)	Ref.
SWCNT	10.61	11.21	1.057	22.73	0.3	1547.5	[206]
	62.2	0.445	0.007	0.763	4.3	1560.1	[207]
	(DW)10.47	1.88	0.18	0.91	2.7	1533.5	[208]
	10.89	3.19	0.29	0.85	3.9	1555.1	
	18.3	0.316	0.017 pJ	0.57	5	1564.5	[209]
	9.8	335	34	12.7	12.1	1563	[210]
	33	3.2	0.097 pJ	0.639	3.9	1559	[211]
	5.7	19.4	3.4	0.18	20.2	1559.6	[212]
	50.4	0.2	0.004	0.9	3	1558	[213]
	42.2	12.5	0.296	0.35	36	1560	[214]
	11.25	8.58	0.763	0.602	4.83	1560	[215]
	22.2	4	0.18	0.51	4.33	1560	[216]
	38.117	11.2	0.3	0.093	42	1560	[217]
BP	5.96	–	–	0.946	2.925	1571.45	[97]
	60.5	–	–	0.280	9.35	1569.24	[218]
	15.22	–	–	1.67	2.4	1567.5	[219]
	5.62	2.23	0.45	1.2	2.2	1560.3	[220]
	30.3	–	–	0.5378	5.33	1567.3	[221]
	23.9	–	–	0.102	40	1555	[222]
	(H)45.9	6.43	0.14	0.100	40	1558	[223]
	5.86	0.3	0.051	0.8	3.25	1561.1	[224]
	23.9	1.7	0.071	0.102	40	1555	[225]
	8.77	–	–	0.67	3.8	1559.5	[43]
Bi_2Se_3	1.21	–	–	1.57	1.79	1564.6	[226]
	12.5	1.8	0.144	0.66	4.3	1557.5	[227]
	5.1 (HML)388	–	–	3.01	0.9	1558.3	[228]
	(HML)239			3.42		1557.4	
				2.02		1559.4	
	(CS)20.27	5.5	0.27	0.908	7.91	1554.56	[205]
	(DS)7.04	75		7.564	26	1559	
	46.4	–	–	0.359	7.76	1597	[229]
	19.352	2	0.0185	1.08	2.8	1530	[230]
	35.45	0.86	0.024	0.36	7.9	–	[231]
	1.71	82.6	48.3	7.78 ns	0.342	1557.908	[153]
Bi_2Te_3	1.7	32.9	19.3	2.7 ns	5.6	1560	[232]
	4.88	5	1.02	1.22	0.95	1558.5	[233]
	15.11	0.8	0.0529	0.6	4.63	1547	[234]
	14.07	–	–	–	4.5	1555.9	[235]
	8.635	–	–	1.08	2.9	1557	[236]
				1.1	3.2		
	1.704	40.37	23.9	3.22 ns	1.696	1558.459	[237]
	18.55	0.5	0.027	0.286	9.15	1560.8	[238]
CoSb3	14.48	–	–	0.833	3.44	1557.9	[239]
MoS_2	5.924	3.5	0.59	1.36	2.7	1570.1	[240]
			–	0.33	7.9	1570	[241]
	11.93	5.85	0.49	0.83	3.5	1571.8	[242]
	29.5	4.13	0.14	0.79	9.5	1574.6	[243]
	11.95	1	–	0.266	10	1561	[244]
	26.02 (CP)33.48	–	–	4.98	23.2	1568	[245]
				0.637	12.38	1568	
MoS_2	6.77	0.065	0.01	–	2.47	1556.86	[246]
	1.927	–	–	0.84	3	–	[247]
	8.968	–	–	1.21	2.1	1530.4	[248]
	14.53	1	0.069	0.2	20.5	1560	[249]
	12.09	–	–	0.71	4	1569.5	[250]

Table 2: (continued)

SA	Repetition rate(MHz)	Output power (mW)	Pulse energy (nJ)	Pulse duration (ps)	3dB bandwidth (nm)	Center wavelength (nm)	Ref.
	463	5.9	–	0.935	6.1	1556.3	[251]
	15.67	9.6	0.61	0.581	4.8	1557.24	[129]
	8.288	–	–	1.28	2.6	1568.9	[252]
MoS_2-WS_2	74.6	19.8	0.27	0.154	24.4	1560	[253]
MoS_2-Sb_2Te_3-MoS_2	36.4	20	0.55	0.286	28	1554	[254]
$MoTe_2$	–	23.4	–	0.1119	24.9	1561	[255]
	5		–	2.57	1.5	1532.5	[256]
	26.601	57	2.14	0.229	11.76	1559.57	[257]
$ReSe_2$	14.97	–	–	0.862	3.4	1561.2	[258]
ReS_2	1.78			3.8	8.2	1563.3	[259]
TiS_2	22.7		0.025	0.812	4.75	1563.3	[260]
Sb_2Te_3	(H)95.4	63	0.66	0.07	63	1542	[261]
	(H)33	9	0.27	0.2	13.3	1568.8	[262]
	22.13	0.9	0.0396	0.449	6	1556	[263]
	25.38	–	0.21	0.167	34	1558	[264]
	31	2	0.06	1.6/(CP)0.197	32.5	–1550	[265]
	4.75	0.5	–	2.02	–	1556	[266]
	22.32	–	–	0.128	30	1565	[267]
	4.75	0.5	0.105	1.8	1.8	1558.6	[268]
	3.75 (HML)304	0.5	133	1.9	1.58	1558	[269]
		4.5	0.014	2.2	1.58	1558.2	
WS_2	31.11	–	–	0.332	8.23	1565	[270]
	25.25	–	–	0.595	5.2	1572	[271]
	–	–	–	1.17	4.16	1563	[272]
	21.07/31.11	0.32/0.43	–	0.457/0.332	5.6/8.23	1566/1565	[273]
	8.05	1.8	0.22	21.1	14.5	1565.5	[274]
	19.58	0.625	–	0.675	–	1558.5	[275]
	19.57	2.64	0.134	0.524	5.19	1563.8	[276]
WSe_2	14.02	–	–	0.477	6.06	1556.42	[203]
WTe_2	13.98	–	–	0.77	4.14	1556.2	[277]
Cu_2S	8.06	4.4	0.545	1.04	3.1	1530.4	[278]
GaSe	8.849	29.1	18.3	4.3	0.83	1555	[279]
GeP	14.82	6.65	0.449	0.722	4.66	1558.29	[280]
rGO	16.79	–	–	1.17	4.04	1544.02	[281]
MgO	3.5	7.6	2.17	5.6	0.24	1569.1	[282]
MXenes	20.0	–	0.065	0.104	42.54	–	[283]
	8.24	–	–	0.946	3.1	1567.3	[284]
	15.4	0.05	–	0.66	5	1557	[32]
	8.25	–	–	5.3	3.4	1565.4	[285]
$PtSe_2$	23.3	–	0.53	1.02	6	1563	[197]
$ReS_{2(1-x)}Se_{2x}$	2.95	0.812	0.275	0.888	4.85	1561.15	[286]
SnS_2	29.3	1.2	0.041	0.623	6.09	1562.01	[287]
SnSe	15.5	0.1	–	0.61	5.27	1559	[288]

HML: harmonic mode locking; CP: after compression; DW: dual-wavelength; H: hybrid mode locking; CS: conventional solitons; DS: dissipative solitons.

5.3 2 μm wavelength mode-locked fiber lasers

Thulium/holmium-doped fiber lasers with operating wavelength of around 2 μm, which is near the absorption peak of water molecules, have attracted much attention for applications in the field of laser surgery, remote sense, laser radar and optoelectronic countermeasures, due to the advantages of high efficiency, easily pump and cavity stability. In recent years, mode-locked Tm-doped fiber lasers (TDF) based on new-type low-dimension materials have been investigated widely. In 2018, Wang et al.

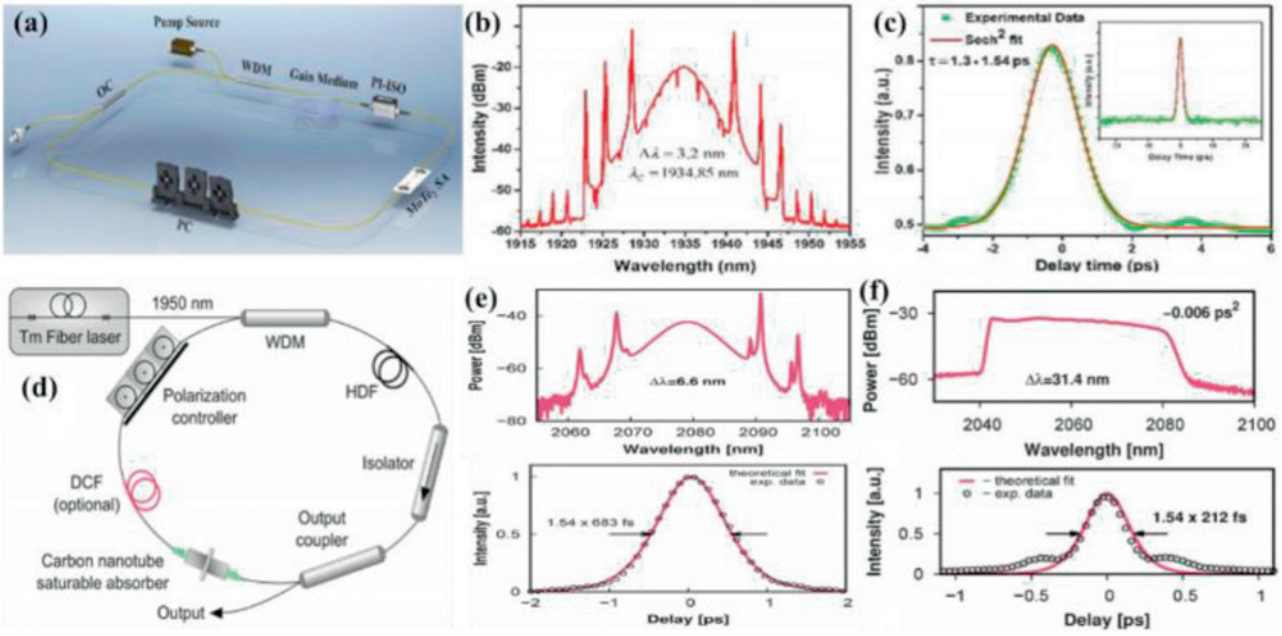

Figure 12: Tm-doped mode-locked fiber laser. (a) Schematic of the passively mode-locked TDF laser based on $MoTe_2$ SA, (b) optical spectrum with the bandwidth of 3.2 nm and (c) autocorrelation trace with a pulse duration of 1.3 ps with $sech^2$ fit (The insert shows the autocorrelation trace with a large range of 50 ps). (d) Setup of the HDF laser based on CNT, (e) performance of the laser operating in the solitonic regime: optical spectrum and pulse autocorrelation and (f) stretched pulse regime: optical spectrum and autocorrelation trace. (a–c) [289], (d–f) [290].

reported Tm-doped mode-locked laser based on $MoTe_2$ SA fabricated by the magnetron sputtering deposition method for the first time. The pulse duration and single pulse energy were 1.3 ps and 13.8 nJ, respectively (Figure 12a–c) [289]. In 2019, Pawliszewska M et al. firstly achieved Ho-doped fiber (HDF) laser operating in anomalous and normal dispersion regime with metallic CNT film fabricated by vacuum filtration technique (Figure 12d–f) [290]. Some important parameters generated by low dimension materials-based Tm/Ho-doped fiber lasers have been listed in Table 3. Similarly, these corresponding data are also shown in Figure 13.

Due to quality beam and small thermal damage, TDF laser based on 2D materials can achieve rapid hemostasis without causing damage to the human body, and therefore is widely used in surgical treatment. There are only a few studies on TDF lasers based on 2D materials, but they all show outstanding performances. We found the ternary TMD SA shows the good performance such as large pulse energy and wide operating wavelength. For example, $ReS_{1.02}Se_{0.9}$ based mode-locked fiber lasers can work at 1.5 and 2 μm wavelength, as shown in Table 3. Figure 12 shows six types of materials that all are able to realize mode locking in 2 μm region. The best one is graphene SA, which can generate the shortest pulses of 205 fs and the highest repetition rate of 58.87 MHz in the Tm/Ho-doped fiber laser. TMDs and TIs SA also present good output characteristics in generating short pulse width. TIs show higher single pulse energy, which is very important for practical applications.

5.4 2~3 μm wavelength mode-locked fiber lasers

Mid-infrared mode-locked lasers have important applications in many fields such as food, medicine, military and molecular fingerprints. The past decade has seen the rapid development of mid-infrared fiber lasers which is driven by the great demand in a wide range of applications including spectroscopy, medical diagnosis, etc. [312, 313]. In particular, Er: ZBLAN (ZrF_4-BaF_2-LaF_3-AlF_3-NaF) fiber lasers at 3 μm have attracted wide attention owing to the advances of fluoride fiber fabrication. Mode-locking operation of an Er-doped ZBLAN fiber laser in the 3 μm wavelength region was first demonstrated by Frerichs and Unrau using the flying mirror technique and an InAs SA [314]. In 2015, Z. Qin et al. reported a passively mode-locked Er:ZBLAN fiber laser based on the mechanically exfoliated BP plated onto the gold-coated mirror, which delivers a maximum average output power of 613 mW, a repetition rate of 24 MHz and a pulse duration of 42 ps, respectively [315]. A mid-infrared

Table 3: Performance summary of mode-locked fiber lasers operating at 2 μm by using various 2D materials as SAs.

SA	Repetition rate (MHz)	Output power (mW)	Pulse energy (nJ)	Pulse duration (ps)	3 dB bandwidth (nm)	Center wavelength (nm)	Ref.
BP	19.2	8.45		1.58	3.9	1898	[291]
	31.8	11	0.345	1.3	4.2	2090	[292]
	36.8	1.5	0.0407	0.739	5.8	1910	[293]
CNT	37	3.4		1.32	5	1932	[294]
	21.05	2.3	0.109	0.973	4.2	1950	[295]
	45		0.5	0.75	6	1885	[296]
	54.52	20.5	0.376	0.683	6.65	2079	[290]
	45	18	0.4	0.45	15.8	1870	[297]
Graphene	6.46	2	0.4	3.6	2.1	1940	[298]
	16.93	1.41	0.081	2.1	2.2	1953.3	[299]
	20.5	1.3		1.2	4	1884	[300]
	41	1.5		0.603	6.6	1876	[301]
	58.87	13	0.22	0.205	27.5	1945	[302]
GO	33.6		4.3	0.59	6.9	1950	[303]
NiO	8.1	7.34		61.27 ns	0.14	1928.81	[304]
Bi_2Te_3	21.5	~2.3		1.26	3.6	1909.5	[305]
	27.9	~1		0.795	5.64	1935	[96]
$CoSb_3$	16.93			0.838	4.62	1912.9	[306]
MoS_2	9.67	150	15.5	843	17.3	1905	[307]
$MoSe_2$	18.21	4.3		0.92	4.62	1912	[308]
$MoTe_2$	15.37	212	13.8	1.3	3.2	1934.85	[257]
WS_2	34.8	0.6	0.0172	1.3	5.6	1941	[309]
WSe_2	11.36	32.5	2.86	1.18	3.29	1886.2	[203]
WTe_2	18.72	39.9	2.13	1.25	3.13	1915.5	[109]
$Ti_3C_2T_x$	13.45	5.8	0.431	2.11	1.86	1862	[310]
$ReS_{1.02}Se_{0.98}$	23.17	313	13.6	1.43	17	1924	[311]

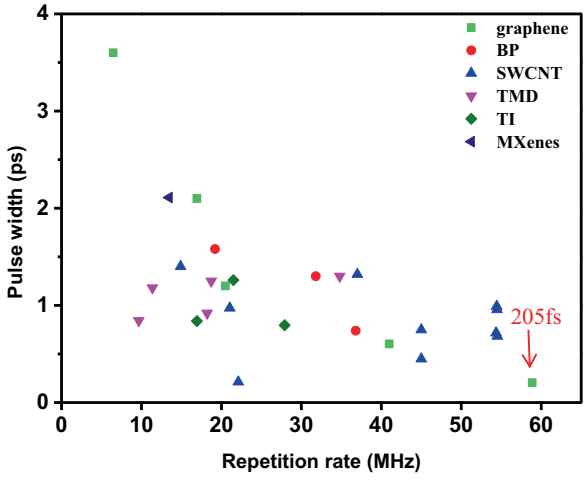

Figure 13: Pulse width versus repetition rate of 2D materials based mode-locked Tm/Ho-fiber lasers (marks with different shapes and colors represent different materials).

mode-locked fluoride fiber laser with Bi_2Te_3 nanosheets as the SA is presented reference [316]. More data for 3 μm mode-locked fiber lasers are listed in Table 4.

Table 4 shows that fewer materials can be used to trigger the mode-locking operation in the Er-doped ZBLAN fiber laser. For the novel 2D materials-based SA, TIs and BP were commonly used and suitable for 3 μm mode-locked fiber lasers due to its ultra-narrow bandgaps. Although BP has excellent performance in the 3 μm wavelength region, the environmental stability of BP is still an obstacle to its photonics applications.

In the above four tables that summarize the applications of 2D materials in ultrafast photonics, the pulse width obtained after additional external compression or through hybrid mode locking has been listed. Generally, the larger dispersion in the cavity, the lower prepetition rate is.On the contrary, the cavity with a higher repetition rate can generate a higher pulse energy.

6 Summary and outlook

In summary, owing to their unique properties, a plenty of emerging 2D materials were explored as SA to realize mode-locked fiber lasers. In this review, we summarize

Table 4: Performance summary of mode-locked fiber lasers operating at ~3 μm by using various 2D materials as SAs.

SA	Repetition rate (MHz)	Output power (mW)	Pulse energy (nJ)	Pulse duration (ps)	3 dB bandwidth (nm)	Center wavelength (nm)	Ref.
BP	27.4	6.2		–	4.9	2771.1	[317]
	28.91	40		–	4.7	3489	[318]
	24.27	613		42	2.8	2783	[315]
	13.98	87.8	6.28	8.6	4.35	2866.7	[319]
Graphene	25.4	18	0.7	42	0.21	2784.5	[320]
Bi_2Te_3	10.4	90	8.6	6	10	2830	[316]

different types of 2D material SAs, according to their operating wavelengths in mode-locked fiber lasers. i) At the 1 μm region, there are plenty of materials can be SAs in the YDF mode-locked lasers, such as graphene, BP, Au-nanotube, SWCNT, Bismuthene, MoS_2, WS_2, SnS_2, Bi_2S_3, Bi_2Se_3 etc. However, some emerging 2D materials are not as good as the mature SWCNT in the Yb-fiber pulses lasers. One can further explore its potential applications in the ultrafast photonics. ii) At the wavelength of 1.5 μm, one can easily fabricate fiber devices by managing the dispersion and the nonlinearity at low cost and with low loss in the fiber cavity. At this case, TMD SA presents better pulse duration and higher repetition rate. iii) At the 2 μm wavelength, the ternary TMD SA shows large pulse energy, wide operating bandwidth. In operation wavelength beyond 3 μm, the BP SA shows the best performance in the mode-locked Er-doped ZBLAN fiber laser.

The outlook about the 2D materials SA in the fiber mode-locked laser field are listed as follows : i) Lucubrating on the applications of mature materials based SAs, such as CNT, graphene and BP, which are able to work at multiple wavelengths including 1, 1.5, 2 μm and even 3 μm in the fiber pulse lasers. ii) Exploring new compound alloy materials or the combination of traditional materials with the emerging materials in order to obtain wider bandwidth, higher damage threshold and lower insert loss. In addition, one can tailor the bandgap for specific wavelength through varying the number of layers of single atom materials and the elemental proportion. In addition, the multi-elemental materials with high damage threshold and wide operation bandwidth are worth investigating, such as ternary TMD family SA. The exploration of potential 2D materials for the commercial product in the mode locked lasers is also crucial issue for the future research. Although many kinds of materials can be used for the ultrafast fiber lasers, there are still not a commercial product like semiconductor saturable absorber mirror (SAM). We believe the research on the multifunctional 2D material SAs for mode-locked fiber lasers will attract much attention in near future.

Acknowledgments: This work was supported by the National Natural Science Foundation of China (61675158), Open Research Fund of State Key Laboratory of Pulsed Laser Technology, and the National Key R&D Program of China (2018YFB1107200).

Author contribution: All the authors have accepted responsibility for the entire content of this submitted manuscript and approved submission.

Research funding: This research was funded by the National Natural Science Foundation of China (61675158), Open Research Fund of State Key Laboratory of Pulsed Laser Technology, and the National Key R&D Program of China (2018YFB1107200).

Employment or leadership: None declared.

Honorarium: None declared.

Conflict of interest statement: The authors declare no conflicts of interest regarding this article.

References

[1] S. Y. Chou, C. Keimel, and J. Gu, "Ultrafast and direct imprint of nanostructures in silicon," *Nature*, vol. 417, pp. 835–837, 2002.

[2] Y. Kondo, K. Nouchi, T. Mitsuyu, M. Watanabe, P. G. Kazansky, and K. Hirao, "Fabrication of long-period fiber gratings by focused irradiation of infrared femtosecond laser pulses," *Opt. Lett.*, vol. 24, pp. 646–648, 1999.

[3] A. Marcinkevičius, S. Juodkazis, M. Watanabe, et al., "Femtosecond laser-assisted three-dimensional microfabrication in silica," *Opt. Lett.*, vol. 26, pp. 277–279, 2001.

[4] C. H. Liu, B. B. Das, W. S. Glassman, et al., "NIR Raman and fluorescence spectroscopies diagnose cancer," *Int. Soc. Optic. Photon.*, vol. 1887, pp. 188–194, 1993.

[5] T. J. Allen, and P. C. Beard, "Mode-locked near-infrared laser diode excitation system for biomedical photoacoustic imaging," *Opt. Lett.*, vol. 31, pp. 3462–3464, 2006.

[6] P. Ajayan, P. Kim, and K. Banerjee, "Two-dimensional van der Waals materials," *Phys. Today*, vol. 69, pp. 9–38, 2016.

[7] B. C. Brodie, "XIII. On the atomic weight of graphite," *Phil. Trans. Roy. Soc. Lond.*, vol. 149, pp. 249–259, 1859.

[8] P. R. Wallace, "The band theory of graphite," *Phys. Rev.*, vol. 71, p. 622, 1947.

[9] K. S. Novoselov, D. Jiang, F. Schedin, et al., "Two-dimensional atomic crystals," *Proc. Natl. Acad. Sci.*, vol. 102, pp. 10451–10453, 2005.
[10] S. Bai, C. Sun, H. Yan, et al., "Healable, transparent, room-temperature electronic sensors based on carbon nanotube network-coated polyelectrolyte multilayers," *Small*, vol. 11, pp. 5807–5813, 2015.
[11] T. Wang, Y. Guo, P. Wan, H. Zhang, X. Chen, and X. Sun, "Flexible transparent electronic gas sensors," *Small*, vol. 12, pp. 3748–3756, 2016.
[12] S. Y. Set, H. Yaguchi, Y. Tanaka, M. Jablonski, "Laser mode locking using a saturable absorber incorporating carbon nanotubes," *J. Lightwave Technol.*, vol. 22, p. 51, 2004.
[13] Z. Wang, Y. Chen, C. Zhao, H. Zhang, and S. Wen, "Switchable dual-wavelength synchronously Q-switched erbium-doped fiber laser based on graphene saturable absorber," *IEEE Photon. J.*, vol. 4, pp. 869–876, 2012.
[14] G. Zheng, Y. Chen, H. Huang, et al., "Improved transfer quality of CVD-grown graphene by ultrasonic processing of target substrates, applications for ultra-fast laser photonics," *ACS Appl. Mater.*, vol. 5, pp. 10288–10293, 2013.
[15] H. Mu, Z. Wang, J. Yuan, et al., "Graphene–Bi_2Te_3 heterostructure as saturable absorber for short pulse generation," *ACS Photonics*, vol. 2, pp. 832–841, 2015.
[16] Q. Bao, H. Zhang, Y. Wang, et al., "Atomic-layer graphene as a saturable absorber for ultrafast pulsed lasers," *Adv. Funct. Mater.*, vol. 19, pp. 3077–3083, 2009.
[17] Y. Ge, Z. Zhu, Y. Xu, et al., "Broadband nonlinear photoresponse of 2D TiS_2 for ultrashort pulse generation and all–optical thresholding devices," *Adv. Opt. Mater.*, vol. 6, 2018, Art no. 1701166.
[18] X. Zhu, S. Chen, M. Zhang, et al., "TiS_2-based saturable absorber for ultrafast fiber lasers," *Photon. Res.*, vol. 6, pp. C44–C48, 2018.
[19] H. Zhang, S. Lu, J. Zheng, et al., "Molybdenum disulfide (MoS_2) as a broadband saturable absorber for ultra-fast photonics," *Optics Express*, vol. 22, pp. 7249–7260, 2014.
[20] M. Liu, Z.-R. Cai, S. Hu, et al., "Dissipative rogue waves induced by long-range chaotic multi-pulse interactions in a fiber laser with a topological insulator-deposited microfiber photonic device," *Opt. Lett.*, vol. 40, pp. 4767–4770, 2015.
[21] Q. Wang, Y. Chen, L. Miao, et al., "Wide spectral and wavelength-tunable dissipative soliton fiber laser with topological insulator nano-sheets self-assembly films sandwiched by PMMA polymer," *Optics Express*, vol. 23, pp. 7681–7693, 2015.
[22] B. Wang, H. Yu, H. Zhang, et al., "Topological insulator simultaneously Q-switched dual-wavelength Nd:Lu_2O_3 laser," *IEEE Photon. J.*, vol. 6, pp. 1–7, 2014.
[23] F. Bernard, H. Zhang, S-P. Gorza, and P. Emplit, Eds. *Towards mode-locked fiber laser using topological insulators. Nonlinear Photonics*, Optical Society of America, 2012.
[24] Z. Chu, J. Liu, Z. Guo, and H. Zhang, "2 μm passively Q-switched laser based on black phosphorus," *Opt. Mater. Express*, vol. 6, pp. 2374–2379, 2016.
[25] J. Du, M. Zhang, Z. Guo, et al., "Phosphorene quantum dot saturable absorbers for ultrafast fiber lasers," *Sci. Rep.*, vol. 7, 2017, Art no. 42357.
[26] X. Chen, G. Xu, X. Ren, et al., "A black/red phosphorus hybrid as an electrode material for high-performance Li-ion batteries and supercapacitors," *Int. J. Mater. Chem. A*, vol. 5, pp. 6581–6588, 2017.
[27] S. Luo, J. Zhao, J. Zou, et al., "Self-standing polypyrrole/black phosphorus laminated film: promising electrode for flexible supercapacitor with enhanced capacitance and cycling stability," *ACS Appl. Mater.*, vol. 10, pp. 3538–3548, 2018.
[28] S. Lu, L. Miao, Z. Guo, et al., "Broadband nonlinear optical response in multi-layer black phosphorus: an emerging infrared and mid-infrared optical material," *Optics Express*, vol. 23, pp. 11183–11194, 2015.
[29] C. Wang, Y. Wang, X. Jiang, et al., "MXene $Ti_3C_2T_x$: a promising photothermal conversion material and application in all-optical modulation and all-optical information loading," *Adv. Opt. Mater.*, vol. 7, 2019, Art no. 1900060.
[30] C. Wang, Y. Wang, X. Jiang, et al., "Thermal stress-induced all-optical modulation in MXene-coated polarization maintaining fiber," *Laser Phys. Lett.*, vol. 16, 2019, Art no. 065107.
[31] J. Liu, X. Jiang, R. Zhang, et al., "MXene-Enabled electrochemical microfluidic biosensor: applications toward multicomponent continuous monitoring in whole blood," *Adv. Funct. Mater.*, vol. 29, 2019, Art no. 1807326.
[32] Y. I. Jhon, J. Koo, B. Anasori, et al., "Metallic MXene saturable absorber for femtosecond mode-locked lasers," *Adv. Mater.*, vol. 29, 2017, Art no. 1702496.
[33] J. Liu, Y. Chen, P. Tang, et al., "Generation and evolution of mode-locked noise-like square-wave pulses in a large-anomalous-dispersion Er-doped ring fiber laser," *Optics Express*, vol. 23, pp. 6418–6427, 2015.
[34] H. Zhang, D. Tang, L. Zhao, and X. Wu, "Dual-wavelength domain wall solitons in a fiber ring laser," *Optics Express*, vol. 19, pp. 3525–3530, 2011.
[35] L. Zhao, D. Tang, X. Wu, H. Zhang, C. Lu, and H. Tam, "Observation of dip-type sidebands in a soliton fiber laser," *Optic Commun.*, vol. 283, pp. 340–343, 2010.
[36] L. Zhao, D. Tang, H. Zhang, T. Cheng, H. Tam, and C. Lu, "Dynamics of gain-guided solitons in an all-normal-dispersion fiber laser," *Opt. Lett.*, vol. 32, pp. 1806–1808, 2007.
[37] Z. Wang, Y. Xu, S. C. Dhanabalan, et al., "Black phosphorus quantum dots as an efficient saturable absorber for bound soliton operation in an erbium doped fiber laser," *IEEE Photon. J.*, vol. 8, pp. 1–10, 2016.
[38] Y. F. Song, H. Zhang, and D. Y. Tang, "Polarization rotation vector solitons in a graphene mode-locked fiber laser," *Optics Express*, vol. 20, pp. 27283–27289, 2012.
[39] Y. Song, Z. Liang, X. Jiang, et al., "Few-layer antimonene decorated microfiber ultra-short pulse generation and all-optical thresholding with enhanced long term stability," *2D Mater.*, vol. 4, 2017, Art no. 045010.
[40] X. Jiang, L. Zhang, S. Liu, et al., "Ultrathin metal–organic framework: an emerging broadband nonlinear optical material for ultrafast photonics," *Adv. Opt. Mater.*, vol. 6, 2018, Art no. 1800561.
[41] P. Li, Y. Chen, T. Yang, et al., "Two-dimensional $CH_3NH_3PbI_3$ perovskite nanosheets for ultrafast mode-locked fiber lasers," *ACS Appl. Mater. Interfaces*, vol. 9, pp. 12759–12765, 2017.
[42] B. Guo, S.-H. Wang, Z.-X. Wu, et al., "Sub-200 fs soliton mode-locked fiber laser based on bismuthene saturable absorber," *Optics Express*, vol. 26, pp. 22750–22760, 2018.
[43] Y. Song, S. Chen, Q. Zhang, et al., "Vector soliton fiber laser passively mode locked by few layer black phosphorus-based

optical saturable absorber," *Optics Express*, vol. 24, pp. 25933–25942, 2016.
[44] X. Jiang, S. Liu, W. Liang, et al., "Broadband nonlinear photonics in few-layer MXene $Ti_3C_2T_x$ (T = F, O, or OH)," *Laser Photon. Rev.*, vol. 12, 2018, Art no. 1700229.
[45] L. Lu, Z. Liang, L. Wu, et al., "Few-layer bismuthene: sonochemical exfoliation, nonlinear optics and applications for ultrafast photonics with enhanced stability," *Laser Photon. Rev.*, vol. 12, 2018, Art no. 1700221.
[46] Y. Zhang, B. Lin, S. C. Tjin, et al., "Refractive index sensing based on higher-order mode reflection of a microfiber Bragg grating," *Optics Express*, vol. 18, pp. 26345–26350, 2010.
[47] J. Zheng, X. Tang, Z. Yang, et al., "Few-Layer phosphorene-decorated microfiber for all-optical thresholding and optical modulation," *Adv. Opt. Mater.*, vol. 5, 2017, Art no. 1700026.
[48] J. Zheng, Z. Yang, C. Si, et al., "Black phosphorus based all-optical-signal-processing: toward high performances and enhanced stability," *ACS Photonics*, vol. 4, pp. 1466–1476, 2017.
[49] Y. Xu, J. Yuan, K. Zhang, et al., "Field-Induced n-doping of black phosphorus for CMOS compatible 2D logic electronics with high electron mobility," *Adv. Funct. Mater.*, vol. 27, 2017, Art no. 1702211.
[50] Z. Guo, S. Chen, Z. Wang, et al., "Metal-ion-modified black phosphorus with enhanced stability and transistor performance," *Adv. Mater.*, vol. 29, 2017, Art no. 1703811.
[51] Z. Huang, W. Han, H. Tang, et al., "Photoelectrochemical-type sunlight photodetector based on MoS_2/graphene heterostructure," *2D Mater.*, vol. 2, 2015, Art no. 035011.
[52] Z. Huang, Z. Zhang, X. Qi, et al., "Wall-like hierarchical metal oxide nanosheet arrays grown on carbon cloth for excellent supercapacitor electrodes," *Nanoscale*, vol. 8, pp. 13273–13279, 2016.
[53] Z. Li, H. Qiao, Z. Guo, et al., "High-performance photo-electrochemical photodetector based on liquid-exfoliated few-layered InSe nanosheets with enhanced stability," *Adv. Funct. Mater.*, vol. 28, 2018, Art no. 1705237.
[54] T. Lv, Y. Li, H. Ma, et al., "Hybrid metamaterial switching for manipulating chirality based on VO2 phase transition," *Sci. Rep.*, vol. 6, 2016, Art no. 23186.
[55] Y. Zhang, C.-K. Lim, Z. Dai, et al., "Photonics and optoelectronics using nano-structured hybrid perovskite media and their optical cavities," *Phys. Rep.*, vol. 795, pp. 1–51, 2019.
[56] X. Ji, N. Kong, J. Wang, et al., "A novel top-down synthesis of ultrathin 2D boron nanosheets for multimodal imaging-guided cancer therapy," *Adv. Mater.*, vol. 30, 2018, Art no. 1803031.
[57] X. Liang, X. Ye, C. Wang, et al., "Photothermal cancer immunotherapy by erythrocyte membrane-coated black phosphorus formulation," *J. Contr. Release*, vol. 296, pp. 150–161, 2019.
[58] M. Qiu, W. X. Ren, T. Jeong, et al., "Omnipotent phosphorene: a next-generation, two-dimensional nanoplatform for multidisciplinary biomedical applications," *Chem. Soc. Rev.*, vol. 47, pp. 5588–5601, 2018.
[59] Z. Sun, Y. Zhao, Z. Li, et al., "TiL_4-Coordinated black phosphorus quantum dots as an efficient contrast agent for in vivo photoacoustic imaging of cancer," *Small*, vol. 13, 2017, Art no. 1602896.
[60] W. Tao, X. Ji, X. Zhu, et al., "Two-dimensional antimonene-based photonic nanomedicine for cancer theranostics," *Adv. Mater.*, vol. 30, 2018, Art no. 1802061.
[61] K. S. Novoselov, A. K. Geim, S. V. Morozov, et al., "Electric field effect in atomically thin carbon films," *Science*, vol. 306, pp. 666–669, 2004.
[62] M. Chernysheva, A. Rozhin, Y. Fedotov, et al., "Carbon nanotubes for ultrafast fibre lasers," *Nanophotonics*, vol. 6, pp. 1–30, 2017.
[63] S. Yamashita. "Nonlinear optics in carbon nanotube, graphene, and related 2D materials," *APL Photonics*, vol. 4, 2019, Art no. 034301.
[64] M. J. Allen, V. C. Tung, and R. B. Kaner, "Honeycomb carbon: a review of graphene," *Chem. Rev.*, vol. 110, pp. 132–145, 2010.
[65] R. R. Nair, P. Blake, A. N. Grigorenko, et al., "Fine structure constant defines visual transparency of graphene," *Science*, vol. 320, p. 1308, 2008.
[66] G. Xing, H. Guo, X. Zhang, T. C. Sum, and C. H. A. Huan, "The physics of ultrafast saturable absorption in graphene," *Optics Express*, vol. 18, pp. 4564–4573, 2010.
[67] D. B. Soh, R. Hamerly, and H. Mabuchi, "Comprehensive analysis of the optical Kerr coefficient of graphene," *Phys. Rev. A*, vol. 94, 2016, Art no. 023845.
[68] Z. Liu, X. Zhang, X. Yan, Y. Chen, and J. Tian, "Nonlinear optical properties of graphene-based materials," *Chin. Sci. Bull.*, vol. 57, pp. 2971–2982, 2012.
[69] B. Radisavljevic, A. Radenovic, J. Brivio, V. Giacometti, and A. Kis, "Single-layer MoS_2 transistors," *Nat. Nanotechnol.*, vol. 6, p. 147, 2011.
[70] Y. Zhang, J. Zhu, P. Li, et al., "All-fiber Yb-doped fiber laser passively mode-locking by monolayer MoS_2 saturable absorber," *Optic Commun.*, vol. 413, pp. 236–241, 2018.
[71] A. Kuc, N. Zibouche, and T. Heine, "Influence of quantum confinement on the electronic structure of the transition metal sulfide TiS_2," *Phys. Rev. B*, vol. 83, 2011, Art no. 245213.
[72] Y. Ding, Y. Wang, J. Ni, L. Shi, S. Shi, and W. Tang, "First principles study of structural, vibrational and electronic properties of graphene-like MX_2 (M= Mo, Nb, W, Ta; X= S, Se, Te) monolayers," *Phys. B: Condensed Matter.*, vol. 406, pp. 2254–2260, 2011.
[73] Q. H. Wang, K. Kalantar-Zadeh, A. Kis, J. N. Coleman, and M. S. Strano, "Electronics and optoelectronics of two-dimensional transition metal dichalcogenides," *Nat. Nanotechnol.*, vol. 7, p. 699, 2012.
[74] S. Kim, A. Konar, W.-S. Hwang, et al., "High-mobility and low-power thin-film transistors based on multilayer MoS_2 crystals," *Nat. Commun.*, vol. 3, pp. 1–7, 2012.
[75] H. Li, Z. Yin, Q. He, et al., "Fabrication of single- and multilayer MoS_2 film-based field-effect transistors for sensing NO at room temperature," *Small*, vol. 8, pp. 63–67, 2011.
[76] Q. Xiang, J. Yu, M. Jaroniec, "Synergetic effect of MoS_2 and graphene as cocatalysts for enhanced photocatalytic H_2 production activity of TiO_2 nanoparticles," *J. Am. Chem. Soc.*, vol. 134, pp. 6575–6578, 2012.
[77] H. S. Lee, S.-W. Min, Y.-G. Chang, et al., "MoS_2 nanosheet phototransistors with thickness-modulated optical energy gap," *Nano Lett.*, vol. 12, pp. 3695–3700, 2012.
[78] Z. Guo, Z. Zhang, S. Lu, et al., "From black phosphorus to phosphorene: basic solvent exfoliation, evolution of Raman scattering, and applications to ultrafast photonics," *Adv. Funct. Mater.*, vol. 25, pp. 6996–7002, 2015.

[79] A. Castellanos-Gomez, L. Vicarelli, E. Prada, et al., "Isolation and characterization of few-layer black phosphorus," *2D Mater.*, vol. 1, 2014, Art no. 025001.
[80] L. Li, Y. Yu, G. J. Ye, et al., "Black phosphorus field-effect transistors," *Nat. Nanotechnol.*, vol. 9, p. 372, 2014.
[81] N. Youngblood, C. Chen, S. J. Koester, and M. Li, "Waveguide-integrated black phosphorus photodetector with high responsivity and low dark current," *Nat. Photon.*, vol. 9, p. 247, 2015.
[82] M. Batmunkh, M. Bat-Erdene, and J. G. Shapter, "Black phosphorus: synthesis and application for solar cells," *Adv. Energy Mater.*, vol. 8, 2018, Art no. 1701832.
[83] M. Z. Hasan, "Colloquium: topological insulators," *Revmodphys*, vol. 82, pp. 3045–3067, 2010.
[84] H. Zhang, C.-X. Liu, X.-L. Qi, X. Dai, Z. Fang, and S.-C. Zhang, "Topological insulators in Bi_2Se_3, Bi_2Te_3 and Sb_2Te_3 with a single dirac cone on the surface," *Nat. Phys.*, vol. 5, pp. 438–442, 2009.
[85] S. Chen, C. Zhao, Y. Li, et al., "Broadband optical and microwave nonlinear response in topological insulator," *Opt. Mater. Express*, vol. 4, pp. 587–596, 2014.
[86] Y. D. Glinka, S. Babakiray, T. A. Johnson, A. D. Bristow, M. B. Holcomb, and D. Lederman, "Ultrafast carrier dynamics in thin-films of the topological insulator Bi_2Se_3," *Appl. Phys. Lett.*, vol. 103, 2013, Art no. 151903.
[87] M. Naguib, V. N. Mochalin, M. W. Barsoum, and Y. Gogotsi, "25th anniversary article: MXenes: a new family of two-dimensional materials," *Adv. Mater.*, vol. 26, pp. 992–1005, 2014.
[88] L. Wang, X. Li, C. Wang, et al., "Few-Layer mxene $Ti_3C_2T_x$ (T= F, O, or OH) for robust pulse generation in a compact Er-doped fiber laser," *ChemNanoMat*, vol. 5, pp. 1233–1238, 2019.
[89] K. Zhu, Y. Jin, F. Du, et al., "Synthesis of Ti_2CT_x MXene as electrode materials for symmetric supercapacitor with capable volumetric capacitance," *J. Energy Chem.*, vol. 31, pp. 11–18, 2019.
[90] Y. Yue, N. Liu, W. Liu, et al., "3D hybrid porous Mxene-sponge network and its application in piezoresistive sensor," *Nano Energy*, vol. 50, pp. 79–87, 2018.
[91] Q. Xue, H. Zhang, M. Zhu, et al., "Photoluminescent Ti_3C_2 MXene quantum dots for multicolor cellular imaging," *Adv. Mater.*, vol. 29, 2017, Art no. 1604847.
[92] J. Yi, L. Du, J. Li, et al., "Unleashing the potential of Ti_2CT_x MXene as a pulse modulator for mid-infrared fiber lasers," *2D Mater.*, vol. 6, 2019, Art no. 045038.
[93] X. Jiang, A. V. Kuklin, A. Baev, et al., "Two-dimensional MXenes: from morphological to optical, electric, and magnetic properties and applications," *Phys. Rep.*, vol. 848, pp. 1–58, 2020.
[94] J. He, L. Tao, H. Zhang, B. Zhou, and J. Li, "Emerging 2D materials beyond graphene for ultrashort pulse generation in fiber lasers," *Nanoscale*, vol. 11, pp. 2577–2593, 2019.
[95] K. Wu, B. Chen, X. Zhang, et al., "High-performance mode-locked and Q-switched fiber lasers based on novel 2D materials of topological insulators, transition metal dichalcogenides and black phosphorus: review and perspective (invited)," *Optic Commun.*, vol. 406, pp. 214–229, 2018.
[96] M. Jung, J. Lee, J. Koo, et al., "A femtosecond pulse fiber laser at 1935 nm using a bulk-structured Bi_2Te_3 topological insulator," *Optics Express*, vol. 22, pp. 7865–7874, 2014.
[97] Y. Chen, G. Jiang, S. Chen, et al., "Mechanically exfoliated black phosphorus as a new saturable absorber for both Q-switching and mode-locking laser operation," *Optics Express*, vol. 23, pp. 12823–12833, 2015.
[98] H. Li, G. Lu, Y. Wang, et al., "Mechanical exfoliation and characterization of single-and few-layer nanosheets of WSe_2, TaS_2, and $TaSe_2$," *Small*, vol. 9, pp. 1974–1981, 2013.
[99] J. Lee, J. Koo, Y. M. Jhon, and J. H. Lee, "A femtosecond pulse erbium fiber laser incorporating a saturable absorber based on bulk-structured Bi_2Te_3 topological insulator," *Optics Express*, vol. 22, pp. 6165–6173, 2014.
[100] K. S. Novoselov, A. K. Geim, S. Morozov, et al., "Two-dimensional gas of massless Dirac fermions in graphene," *Nature*, vol. 438, pp. 197–200, 2005.
[101] D. Anderson, M. Desaix, M. Karlsson, M. Lisak, and M. Quiroga-Teixeiro, "Wave-breaking-free pulses in nonlinear-optical fibers," *J. Opt. Soc. Am. B*, vol. 10, pp. 1185–1190, 1993.
[102] Z. Wang, H. Jia, X. Zheng, et al., "Black phosphorus nanoelectromechanical resonators vibrating at very high frequencies," *Nanoscale*, vol. 7, pp. 877–884, 2015.
[103] M. C. Valeria Nicolosi, M. G. Kanatzidis, M. S. Strano, and J. N. Coleman, "Liquid exfoliation of layered materials," *Science*, vol. 340, 2013, Art no. 1226419.
[104] F. Bonaccorso and Z. Sun, "Solution processing of graphene, topological insulators and other 2d crystals for ultrafast photonics," *Opt. Mater. Express*, vol. 4, p. 63, 2013.
[105] E. J. Aiub, D. Steinberg, E. A. T. de Souza, and L. A. Saito, "200-fs mode-locked Erbium-doped fiber laser by using mechanically exfoliated MoS_2 saturable absorber onto D-shaped optical fiber," *Optics Express*, vol. 25, pp. 10546–10552, 2017.
[106] Z.-C. Luo, M. Liu, Z.-N. Guo, et al., "Microfiber-based few-layer black phosphorus saturable absorber for ultra-fast fiber laser," *Optics Express*, vol. 23, pp. 20030–20039, 2015.
[107] X. Li, W. Cai, J. An, et al., "Large-area synthesis of high-quality and uniform graphene films on copper foils," *Science*, vol. 324, pp. 1312–1314, 2009.
[108] W. Liu, M. Liu, J. Yin, et al., "Tungsten diselenide for all-fiber lasers with the chemical vapor deposition method," *Nanoscale*, vol. 10, pp. 7971–7977, 2018.
[109] J. Wang, Z. Jiang, H. Chen, et al., "Magnetron-sputtering deposited WTe_2 for an ultrafast thulium-doped fiber laser," *Opt. Lett.*, vol. 42, pp. 5010–5013, 2017.
[110] Q. Bao, H. Zhang, Y. Wang, et al., "Atomic-layer graphene as a saturable absorber for ultrafast mode-locked lasers," *Adv. Funct. Mater.*, vol. 19, pp. 3077–3083, 2009.
[111] J. Yin, J. Li, H. Chen, et al., "Large-area highly crystalline WSe_2 atomic layers for ultrafast mode-locked lasers," *Optics Express*, vol. 25, pp. 30020–30031, 2017.
[112] K. Kashiwagi, S. Yamashita, and S. Y. Set, "Optically manipulated deposition of carbon nanotubes onto optical fiber end," *Jpn. J. Appl. Phys.*, vol. 46, p. L988, 2007.
[113] Y. Zhou, R. Zhang, P. Chen, et al., "Passively Q-switched and mode-locked ytterbium fiber laser with Bi_2S_3 nanowire," *Laser Phys.*, vol. 29, 2019, Art no. 055101.
[114] J. Lee, J. Koo, J. Lee, Y. M. Jhon, and J. H. Lee, "All-fiberized, femtosecond laser at 1912 nm using a bulk-like $MoSe_2$ saturable absorber," *Opt. Mater. Express*, vol. 7, pp. 2968–2979, 2017.
[115] H. Liu, A.-P. Luo, F.-Z. Wang, et al., "Femtosecond pulse erbium-doped fiber laser by a few-layer MoS_2 saturable absorber," *Opt. Lett.*, vol. 39, pp. 4591–4594, 2014.

[116] K. Wu, X. Zhang, J. Wang, and J. Chen, "463-MHz fundamental mode-locked fiber laser based on few-layer MoS_2 saturable absorber," *Opt. Lett.*, vol. 40, pp. 1374–1377, 2015.
[117] L. Li, S. Jiang, Y. Wang, et al., "WS_2/fluorine mica (FM) saturable absorbers for all-normal-dispersion mode-locked fiber laser," *Optics Express*, vol. 23, pp. 28698–28706, 2015.
[118] K. Wu, X. Zhang, J. Wang, X. Li, and J. Chen, "WS_2 as a saturable absorber for ultrafast photonic applications of mode-locked and Q-switched lasers," *Optics Express*, vol. 23, pp. 11453–11461, 2015.
[119] W. Liu, M. Liu, H. Han, et al., "Nonlinear optical properties of WSe_2 and $MoSe_2$ films and their applications in passively Q-switched erbium doped fiber lasers," *Photon. Res.*, vol. 6, pp. C15–C21, 2018.
[120] W. Liu, M. Liu, Y. OuYang, H. Hou, M. Lei, and Z. Wei, "CVD-grown $MoSe_2$ with high modulation depth for ultrafast mode-locked erbium-doped fiber laser," *Nanotechnology*, vol. 29, 2018, Art no. 394002.
[121] R. Khazaeizhad, S. H. Kassani, H. Jeong, D.-I. Yeom, and K. Oh, "Mode-locking of Er-doped fiber laser using a multilayer MoS_2 thin film as a saturable absorber in both anomalous and normal dispersion regimes," *Optics Express*, vol. 22, pp. 23732–23742, 2014.
[122] P. Yan, H. Chen, J. Yin, et al., "Large-area tungsten disulfide for ultrafast photonics," *Nanoscale*, vol. 9, pp. 1871–1877, 2017.
[123] Q. Guo, Y. Cui, Y. Yao, et al., "A solution-processed ultrafast optical switch based on a nanostructured epsilon-near-zero medium." *Adv. Mater.*, vol. 29, 2017, Art no. 1700754.
[124] X. Han, "2D $MoTe_2$ film as a saturable absorber for a wavelength-tunable ultrafast fiber laser," *Appl. Optic.*, vol. 58, pp. 8390–8395, 2019.
[125] R. Lü, Y. Wang, J. Wang, et al., "Soliton and bound-state soliton mode-locked fiber laser based on a MoS_2/fluorine mica Langmuir–Blodgett film saturable absorber," *Photon. Res.*, vol. 7, pp. 431–436, 2019.
[126] Y.-W. Song, S. Yamashita, C. S. Goh, and S. Y. Set, "Carbon nanotube mode lockers with enhanced nonlinearity via evanescent field interaction in D-shaped fibers," *Opt. Lett.*, vol. 32, pp. 148–150, 2007.
[127] Y-W. Song, K. Morimune, S. Y. Set, and S. Yamashita, "Polarization insensitive all-fiber mode-lockers functioned by carbon nanotubes deposited onto tapered fibers," *Appl. Phys. Lett.*, vol. 90, 2007, Art no. 021101.
[128] W. Li, B. Chen, C. Meng, et al., "Ultrafast all-optical graphene modulator," *Nano Lett.*, vol. 14, pp. 955–959, 2014.
[129] E. J. Lee, S. Y. Choi, H. Jeong, et al., "Active control of all-fibre graphene devices with electrical gating," *Nat. Commun.*, vol. 6, p. 6851, 2015.
[130] S. Yu, X. Wu, Y. Wang, X. Guo, and L. Tong, "2D materials for optical modulation: challenges and opportunities," *Adv. Mater.*, vol. 29, 2017, Art no. 1606128.
[131] J. Wang, L. Chen, C. Dou, H. Yan, L. Meng, and Z. Wei, "$Mo_{0.5}W_{0.5}S_2$ for Q-switched pulse generation in ytterbium-doped fiber laser," *Nanotechnology*, vol. 29, 2018, Art no. 224002.
[132] T. Jiang, K. Yin, C. Wang, et al., "Ultrafast fiber lasers mode-locked by two-dimensional materials: review and prospect," *Photon. Res.*, vol. 8, p. 78, 2019.
[133] Z.-B. Liu, X. He, and D. Wang, "Passively mode-locked fiber laser based on a hollow-core photonic crystal fiber filled with few-layered graphene oxide solution," *Opt. Lett.*, vol. 36, pp. 3024–3026, 2011.
[134] J. Zhao, S. Ruan, P. Yan, et al., "Cladding-filled graphene in a photonic crystal fiber as a saturable absorber and its first application for ultrafast all-fiber laser," *Opt. Eng.*, vol. 52, 2013, Art no. 106105.
[135] Y. Peiguang, L. Rongyong, C. Hao, et al., "Topological insulator solution filled in photonic crystal fiber for passive mode-locked fiber laser," *IEEE Photon. Technol. Lett.*, vol. 27, pp. 264–267, 2015.
[136] P. Yan, A. Liu, Y. Chen, et al., "Passively mode-locked fiber laser by a cell-type WS_2 nanosheets saturable absorber," *Sci. Rep.*, vol. 5, 2015, Art no. 12587.
[137] X. Li, M. Liu, Z. Yan, et al., Eds. All-fiber all-normal-dispersion passively mode-locked Yb-doped ring laser based on graphene oxide. *2012 Photonics Global Conference (PGC)*, IEEE; 2012.
[138] H. Liu, X. W. Zheng, M. Liu, et al., "Femtosecond pulse generation from a topological insulator mode-locked fiber laser," *Optics Express*, vol. 22, pp. 6868–6873, 2014.
[139] M. Ma, W. Wen, Y. Zhang, et al., "Few-layer $ReS_{2(1-x)}Se_{2x}$ nanoflakes for noise-like pulse generation in a mode-locked ytterbium-doped fiber laser," *Int. J. Mater. Chem. C*, vol. 7, pp. 6900–6904, 2019.
[140] H. R. Chen, C. Y. Tsai, H. M. Cheng, K. H. Lin, and W. F. Hsieh, "Passive mode locking of ytterbium- and erbium-doped all-fiber lasers using graphene oxide saturable absorbers," *Optics Express*, vol. 22, pp. 12880–12889, 2014.
[141] Z. Cheng, H. Li, H. Shi, J. Ren, Q. H. Yang, and P. Wang, "Dissipative soliton resonance and reverse saturable absorption in graphene oxide mode-locked all-normal-dispersion Yb-doped fiber laser," *Optics Express*, vol. 23, pp. 7000–7006, 2015.
[142] S. Huang, Y. Wang, Y. Peiguang, et al., "Observation of multipulse bunches in a graphene oxide passively mode-locked ytterbium-doped fiber laser with all-normal dispersion," *Appl. Phys. B*, vol. 116, pp. 939–946, 2014.
[143] S. Huang, Y. Wang, P. Yan, J. Zhao, H. Li, and R. Lin, "Tunable and switchable multi-wavelength dissipative soliton generation in a graphene oxide mode-locked Yb-doped fiber laser," *Optics Express*, vol. 22, pp. 11417–11426, 2014.
[144] R.-Y. Lin, Y.-G. Wang, P.-G. Yan, et al., "Bright and dark square pulses generated from a graphene-oxide mode-locked ytterbium-doped fiber laser," *IEEE Photon. J.*, vol. 6, pp. 1-8, 2014.
[145] N. Zhao, M. Liu, H. Liu, et al., "Dual-wavelength rectangular pulse Yb-doped fiber laser using a microfiber-based graphene saturable absorber," *Optics Express*, vol. 22, pp. 10906–10913, 2014.
[146] F. Bo, H. Yi, X. Xiao, H. Zhu, Z. Sun, and C. Yang, "Broadband graphene saturable absorber for pulsed fiber lasers at 1, 1.5, and 2 μm," *IEEE J. Sel. Top. Quant. Electron.*, vol. 20, pp. 411–415.
[147] L. Jiang, S. Wu, Q. H. Yang, and W. Pu, "Mode-locked and Q-switched Yb-doped fiber lasers with graphene saturable absorber," in *Proceedings of Spie the International Society for Optical Engineering*, 2011.
[148] L. Jiang, W. Rusheng, X. Jia, X. Xiangang, and W. Pu, "Passively mode-locked Yb-doped fiber laser with graphene epitaxially

grown on 6H-SiC substrates," *Chin. J. Lasers*, vol. 38, 2011, Art no. 0802003.
[149] H.-R. Chen, C.-Y. Tsai, K.-H. Lin, J.-Y. Wang, and W.-F. Hsieh, Eds. Stable and self-starting passively mode-locked fiber laser for 1.06 μm and 1.55 μm by using graphene oxide saturable absorber. *Conference on Lasers and Electro-Optics/Pacific Rim*. Optical Society of America, 2013.
[150] L. Zhao, D. Tang, H. Zhang, X. Wu, Q. Bao, and K. P. Loh, "Dissipative soliton operation of an ytterbium-doped fiber laser mode locked with atomic multilayer graphene," *Opt. Lett.*, vol. 35, pp. 3622–3624, 2010.
[151] S. S. Huang, Y. G. Wang, H. Q. Li, et al., "Experimental study on the multi-pulse phenomenon of graphene oxide passively mode-locked erbium-doped fiber lasers," *Acta Phys. Sin.*, vol. 63, pp. 84202–084202, 2014.
[152] Y. Li, Y. He, Y. Cai, et al., "Black phosphorus: broadband nonlinear optical absorption and application," *Laser Phys. Lett.*, vol. 15, 2018. https://doi.org/10.1088/1612-202X/aa94e3.
[153] Q. Guo, J. Pan, Y. Liu, et al., "Output energy enhancement in a mode-locked Er-doped fiber laser using CVD-Bi_2Se_3 as a saturable absorber," *Optics Express*, vol. 27, pp. 24670–24681, 2019.
[154] D. Wang, H. Song, X. Long, and L. Li, "Switchable and tunable multi-wavelength emissions in mode-locked ytterbium fiber lasers with black phosphorus saturable absorbers and polarization-maintaining fiber Bragg gratings," *Optic Commun.*, vol. 452, pp. 373–379, 2019.
[155] P. Guo, X. Li, T. Chai, et al., "Few-layer bismuthene for robust ultrafast photonics in C-Band optical communications," *Nanotechnology*, vol. 30, 2019, Art no. 354002.
[156] J. Lee, J. Koo, and J. H. Lee, "Femtosecond mode-locking of an ytterbium-doped fiber laser using self-assembled gold nanorods," *Laser Phys. Lett.*, vol. 14, 2017. https://doi.org/10.1088/1612-202X/aa7d7a.
[157] X. Li, Y. Wang, Y. Wang, et al., "Nonlinear absorption of SWNT film and its effects to the operation state of pulsed fiber laser," *Optics Express*, vol. 22, pp. 17227–17235, 2014.
[158] L. Hou, H. Guo, Y. Wang, et al., "Sub-200 femtosecond dispersion-managed soliton ytterbium-doped fiber laser based on carbon nanotubes saturable absorber," *Optics Express*, vol. 26, pp. 9063–9070, 2018.
[159] H. Guo, L. Hou, Y. Wang, et al., "Tunable ytterbium-doped mode-locked fiber laser based on single-walled carbon nanotubes," *J. Lightwave Technol.*, vol. 37, pp. 2370–2374, 2019.
[160] Z. Zhang, D. Popa, V. J. Wittwer, et al., "All-fiber nonlinearity- and dispersion-managed dissipative soliton nanotube mode-locked laser," *Appl. Phys. Lett.*, vol. 107, 2015, Art no. 241107.
[161] C. S. Goh, K. Kikuchi, S. Y. Set, et al., Eds, Femtosecond mode-locking of a ytterbium-doped fiber laser using a carbon-nanotube-based mode-locker with ultra-wide absorption band. *(CLEO) Conference on Lasers and Electro-Optics, 2005*. IEEE, 2005.
[162] X. Li, Y. Wang, Y. Wang, et al., "Nonlinear absorption of SWNT film and its effects to the operation state of pulsed fiber laser," *Optics Express*, vol. 22, 2014, Art no. 17227.
[163] L. N. Duan, L. Li, Y. G. Wang, and X. Wang, "All-fiber dissipative soliton laser based on single-walled carbon nanotube absorber in normal dispersion regime," *Optik*, vol. 137, pp. 308–312, 2017.
[164] L. Li, Y. Wang, H. Sun, L. Duan, X. Wang, and J. Si, "Single-walled carbon nanotube solution-based saturable absorbers for mode-locked fiber laser," *Opt. Eng.*, vol. 54, 2015, https://doi.org/10.1117/1.oe.54.8.086103.
[165] L. Xiao-Hui, W. Yong-Gang, W. Yi-Shan, et al., "Wavelength-Switchable and wavelength-tunable all-normal-dispersion mode-locked Yb-doped fiber laser based on single-walled carbon nanotube wall paper absorber," *IEEE Photon. J.*, vol. 4, pp. 234–241, 2012.
[166] Z. Kang, Y. Xu, Z. X. Jia, G. S. Qin, and W. P. Qin, "0.8 nm single wall carbon nanotubes for wideband ultrafast pulse generation," *Laser Phys.*, vol. 26, 2016, https://doi.org/10.1088/1054-660x/26/4/045102.
[167] S. M. Kobtsev, S. V. Kukarin, and Y. S. Fedotov, "Mode-locked Yb-fiber laser with saturable absorber based on carbon nanotubes," *Laser Phys.*, vol. 21, pp. 283–286, 2011.
[168] X. Li, Y. Wang, Y. Wang, et al., "Yb-doped passively mode-locked fiber laser based on a single wall carbon nanotubes wallpaper absorber," *Optics Laser. Technol.*, vol. 47, pp. 144–147, 2013.
[169] Y. B. Wang, X. H. Qi, Y. Shen, et al., "Ultra-long cavity carbon nanotube mode-locked multi-wavelength erbium-doped fiber laser," *Chin. J. Phys.*, vol. 64, 2015, Art no. 204205.
[170] S. S. Wang, Y. Z. Pan, and R. X. Gao, "Mode-locked double-clad fiber laser with a carbon nanotubes saturable absorber," *Acta Phys. Sin.*, vol. 62, 2013, Art no. 024209.
[171] K. Kieu and F. Wise, "All-fiber normal-dispersion femtosecond laser," *Optics Express*, vol. 16, pp. 11453–11458, 2008.
[172] T. Chai, X. Li, T. Feng, et al., "Few-layer bismuthene for ultrashort pulse generation in a dissipative system based on an evanescent field," *Nanoscale*, vol. 10, pp. 17617–17622, 2018.
[173] S. Sathiyan, V. Velmurugan, K. Senthilnathan, P. Ramesh Babu, and S. Sivabalan, "All-normal dispersion passively mode-locked Yb-doped fiber laser using MoS_2–PVA saturable absorber," *Laser Phys.*, vol. 26, 2016, https://doi.org/10.1088/1054-660x/26/5/055103.
[174] H. Lee, "Monolayer MoS_2-based high energy rectangular pulse fiber laser," *Optik*, vol. 174, pp. 530–536, 2018.
[175] D. Mao, S. Zhang, Y. Wang, et al., "WS_2 saturable absorber for dissipative soliton mode locking at 1.06 and 1.55 microm," *Optics Express*, vol. 23, pp. 27509–27519, 2015.
[176] H. Guoyu, K. Li, Z. Dong, et al., "Characteristics of WS_2 mode-locked Yb-doped fiber laser." in *Fifth International Symposium on Laser Interaction with Matter*, 2019.
[177] J. Li, Y. Zhao, Q. Chen, K. Niu, R. Sun, and H. Zhang, "Passively mode-locked ytterbium-doped fiber laser based on SnS_2 as saturable absorber," *IEEE Photon. J.*, vol. 9, pp. 1–7, 2017.
[178] H. R. Yang and X. M. Liu, "Nonlinear optical response and applications of tin disulfide in the near- and mid-infrared," *Appl. Phys. Lett.*, vol. 110, 2017. https://doi.org/10.1063/1.4982624.
[179] J. Gao, J. Pan, Y. Liu, et al., "Observation of the dispersion effect of SnS_2 nanosheets in all-normal-dispersion Yb-doped mode-locked fiber laser," *Infrared Phys. Technol.*, vol. 102, 2019. https://doi.org/10.1016/j.infrared.2019.102982.
[180] Y. Zhou, R. Zhang, P. Chen, et al., "Passively Q-switched and mode-locked ytterbium fiber laser with Bi_2S_3 nanowire," *Laser*

Phys., vol. 29, 2019. https://doi.org/10.1088/1555-6611/aaff59.

[181] Z. Dou, Y. Song, J. Tian, J. Liu, Z. Yu, and X. Fang, "Mode-locked ytterbium-doped fiber laser based on topological insulator: Bi_2Se_3," *Optics Express*, vol. 22, pp. 24055–24061, 2014.

[182] K. Li, J. Tian, Y. Song, et al., "Bi_2Se_3 as a saturable absorber for ultrafast photonic applications of Yb-doped fiber lasers," *Opt. Eng.*, vol. 55, 2016. https://doi.org/10.1117/1.OE.55.3.036110.

[183] J.-H. Lin, G.-H. Huang, C.-H. Ou, et al., "Q-switched pulse and mode-locked pulse generation from a Yb^{3+}-doped fiber laser based on Bi_2Se_3," *IEEE Photon. J.*, vol. 10, pp. 1–10, 2018.

[184] X. Han, H. Zhang, C. Zhang, et al., "Large-energy mode-locked ytterbium-doped linear-cavity fiber laser based on chemical vapor deposition-Bi_2Se_3 as a saturable absorber," *Appl. Optic.*, vol. 58, pp. 2695–2701, 2019.

[185] C. Chi, J. Lee, J. Koo, and J. Han Lee, "All-normal-dispersion dissipative-soliton fiber laser at 1.06 μm using a bulk-structured Bi_2Te_3 topological insulator-deposited side-polished fiber," *Laser Phys.*, vol. 24, 2014. https://doi.org/10.1088/1054-66/24/10/105106.

[186] L. Li, P.-G. Yan, Y.-G. Wang, L.-N. Duan, H. Sun, and J.-H. Si, "Yb-doped passively mode-locked fiber laser with Bi_2Te_3-deposited," *Chin. Phys. B*, vol. 24, 2015. https://doi.org/10.1088/1674-1056/24/12/124204.

[187] L. Li, Y. Wang, X. Wang, T. Lin, and H. Sun. "High energy mode-locked Yb-doped fiber laser with Bi_2Te_3 deposited on tapered-fiber," *Optik*, vol. 142, pp. 470–474, 2017.

[188] Z. Wang, H. Mu, C. Zhao, Q. Bao, and H. Zhang. "Harmonic mode-locking and wavelength-tunable Q-switching operation in the graphene–Bi_2Te_3 heterostructure saturable absorber-based fiber laser," *Opt. Eng.* vol. 55, 2016. https://doi.org/10.1117/1.OE.55.8.081314.

[189] Z. Wang, H. Mu, J. Yuan, C. Zhao, Q. Bao, and H. Zhang, "Graphene-Bi_2Te_3 heterostructure as broadband saturable absorber for ultra-short pulse generation in Er-doped and Yb-doped fiber lasers," *IEEE J. Sel. Top. Quant. Electron.*, vol. 23, pp. 195–199, 2017.

[190] M. Kowalczyk, J. Bogusławski, R. Zybała, et al., "Sb_2Te_3-deposited D-shaped fiber as a saturable absorber for mode-locked Yb-doped fiber lasers," *Opt. Mater. Express*, vol. 6, 2016, https://doi.org/10.1364/ome.6.002273.

[191] M. Kowalczyk, J. Bogusławski, R. Zybała, et al., "Sb_2Te_3-deposited D-shaped fiber as a saturable absorber for mode-locked Yb-doped fiber lasers," *Opt. Mater. Express*, vol. 6, 2016, https://doi.org/10.1364/ome.6.002273.

[192] J. I. Mackenzie, H. JelÍnková, T. Taira, et al., "All-normal dispersion Yb-doped fiber laser mode-locked by Sb_2Te_3 topological insulator," in *Laser Sources and Applications III*, 2016.

[193] J. Yuan, H. Mu, L. Li, et al., "Few-layer platinum diselenide as a new saturable absorber for ultrafast fiber lasers," *ACS Appl. Mater. Interfaces*, vol. 10, pp. 21534–21540, 2018.

[194] J. He, Y. Li, Y. Lou, G. Zeng, and L. Tao, "Optical deposition of $PtSe_2$ on fiber end face for Yb-doped mode-locked fiber laser," *Optik*, vol. 198, 2019, https://doi.org/10.1016/j.ijleo.2019.163298.

[195] N. Xu, W. Yang, and H. Zhang, "Nonlinear saturable absorption properties of indium selenide and its application for demonstrating a Yb-doped mode-locked fiber laser," *Opt. Mater. Express*, vol. 8, 2018, https://doi.org/10.1364/ome.8.003092.

[196] H. Long, Y. Shi, Q. Wen, and Y. H. Tsang, "Ultrafast laser pulse (115 fs) generation by using direct bandgap ultrasmall 2D GaTe quantum dots," *Int. J. Mater. Chem. C*, vol. 7, pp. 5937–5944, 2019.

[197] Y. Shi, H. Long, S. Liu, Y. H. Tsang, and Q. Wen, "Ultrasmall 2D NbSe2 based quantum dots used for low threshold ultrafast lasers," *Int. J. Mater. Chem. C*, vol. 6, pp. 12638–12642, 2018.

[198] M. Tuo, C. Xu, H. Mu, et al., "Ultrathin 2D transition metal carbides for ultrafast mode-locked fiber lasers," *ACS Photonics*, vol. 5, pp. 1808–1816, 2018.

[199] Y. Ge, W. Huang, F. Yang, et al., "Beta-lead oxide quantum dot (beta-PbO QD)/polystyrene (PS) composite films and their applications in ultrafast photonics," *Nanoscale*, vol. 11, pp. 6828–6837, 2019.

[200] J. Liu, X. Li, Y. Xu, et al., "$NiPS_3$ nanoflakes: a nonlinear optical material for ultrafast photonics," *Nanoscale*, vol. 11, pp. 14383–14391, 2019.

[201] X. Bao, H. Mu, Y. Chen, et al., "Ytterbium-doped fiber laser passively mode locked by evanescent field interaction with $CH_3NH_3SnI_3$ perovskite saturable absorber," *J. Phys. D: Appl. Phys.*, vol. 51, 2018, https://doi.org/10.1088/1361-6463/aad71d.

[202] J. Yi, L. Du, J. Li, et al., "Unleashing the potential of Ti_2CT_x MXene as a pulse modulator for mid-infrared fiber lasers," *2D Mater.*, vol. 6, 2019, https://doi.org/10.1088/2053-1583/ab39bc.

[203] H. Jeong, S. Y. Choi, F. Rotermund, Y. H. Cha, D. Y. Jeong, and D. I. Yeom, "All-fiber mode-locked laser oscillator with pulse energy of 34 nJ using a single-walled carbon nanotube saturable absorber," *Optics Express*, vol. 22, pp. 22667–22672, 2014.

[204] J. Yin, J. Li, H. Chen, et al., "Large-area highly crystalline WSe_2 atomic layers for ultrafast pulsed lasers," *Optics Express*, vol. 25, pp. 30020–30031, 2017.

[205] H. Song, J. Liu, B. Liu, J. Wu, H.-M. Cheng, and F. Kang, "Two-dimensional materials for thermal management applications," *Joule*, vol. 2, pp. 442–463, 2018.

[206] Y. Zhou, J. Lin, X. Zhang, et al., "Self-starting passively mode-locked all fiber laser based on carbon nanotubes with radially polarized emission," *Photon. Res.*, vol. 4, 2016, https://doi.org/10.1364/prj.4.000327.

[207] K. Wu, X. Li, Y. Wang, Q. J. Wang, P. P. Shum, and J. Chen, "Towards low timing phase noise operation in fiber lasers mode locked by graphene oxide and carbon nanotubes at 1.5 μm," *Optics Express*, vol. 23, pp. 501–511, 2015.

[208] K. Y. Lau, P. J. Ker, A. F. Abas, M. T. Alresheedi, and M. A. Mahdi, "Mode-locked fiber laser in the C-band region for dual-wavelength ultrashort pulses emission using a carbon nanotube saturable absorber," *Chinese Opt. Lett.*, vol. 17, 2019, Art no. 051401.

[209] S. R. Yemineni, A. Arokiaswami, and P. Shum, Eds. All-fiber femtosecond laser pulse generation at 1.55 μm and 2 μm using a common carbon-nanotube based saturable absorber. *2017 Conference on Lasers and Electro-Optics Pacific Rim (CLEO-PR)*. IEEE, 2017.

[210] H. Jeong, S. Y. Choi, F. Rotermund, Y.-H. Cha, D.-Y. Jeong, and D.-I. Yeom, "All-fiber mode-locked laser oscillator with pulse

energy of 34 nJ using a single-walled carbon nanotube saturable absorber," *Optics Express*, vol. 22, pp. 22667–22672, 2014.

[211] T. Jiang, Z. Kang, G. Qin, J. Zhou, and W. Qin. "Low mode-locking threshold induced by surface plasmon field enhancement of gold nanoparticles," *Optics Express*, vol. 21, pp. 27992–8000, 2013.

[212] J. H. Kim, H. Lee, C. D. T. Nguyen, K.-S. Kim, and S. Kim, Eds, Broadband 3.4 nJ pulse generation using a fiber laser mode-locked by composite-type carbon nanotubes saturable absorber. *Bragg Gratings, Photosensitivity, and Poling in Glass Waveguides*. Optical Society of America, 2014.

[213] S. Yamashita, Y. Inoue, S. Maruyama, et al., "Saturable absorbers incorporating carbon nanotubes directly synthesized onto substrates and fibers and their application to mode-locked fiber lasers," *Opt. Lett.*, vol. 29, pp. 1581–1583, 2004.

[214] D. A. Dvoretskiy, S. G. Sazonkin, I. O. Orekhov, et al., Eds, Ultrafast all-fiber erbium-doped ring laser mode-locked by high-density well-aligned single-walled carbon nanotubes. *2017 Conference on Lasers and Electro-Optics Europe & European Quantum Electronics Conference (CLEO/Europe-EQEC)*. IEEE, 2017.

[215] H. Jeong, S. Y. Choi, E. I. Jeong, S. J. Cha, F. Rotermund, and D. I. Yeom, "Ultrafast mode-locked fiber laser using a waveguide-type saturable absorber based on single-walled carbon nanotubes," *Appl. Phys. Express*, vol. 6, 2013, Art no. 052705.

[216] H. Jeong, Y. C. Sun, F. Rotermund, K. Lee, and D. I. Yeom, "All-polarization maintaining passively mode-locked fiber laser using evanescent field interaction with single-walled carbon nanotube saturable absorber," *J. Lightwave Technol.*, vol. 34, pp. 3510–3514, 2016.

[217] V. Lazarev, A. Krylov, D. Dvoretskiy, et al., "Stable similariton generation in an all-fiber hybrid mode-locked ring laser for frequency metrology," *IEEE Trans. Ultrason. Ferroelectrics Freq. Contr.*, vol. 63, pp. 1028–1033, 2016.

[218] Y. Chen, S. Chen, J. Liu, Y. Gao, and W. Zhang. "Sub-300 femtosecond soliton tunable fiber laser with all-anomalous dispersion passively mode locked by black phosphorus," *Optics Express*, vol. 24, pp. 13316–13324, 2016.

[219] Y. Xu, Z. Wang, Z. Guo, et al., "Solvothermal synthesis and ultrafast photonics of black phosphorus quantum dots," *Adv. Opt. Mater.*, vol. 4, pp. 1223–1229, 2016.

[220] J. Du, M. Zhang, X. Zhu, et al., Eds. Microfiber-based few-layer black phosphorus quantum dots saturable absorber for mode-locked fiber laser. *2016 Conference on Lasers and Electro-Optics (CLEO)*. IEEE, 2016.

[221] X. Jin, G. Hu, M. Zhang, et al., Eds. Stable, Inkjet printed temperature-and humidity-resistant black phosphorus for ultrafast lasers. *CLEO: Science and Innovations*. Optical Society of America, 2018.

[222] X. Jin, G. Hu, M. Zhang, et al., Eds. Ultrafast dispersion-managed fiber laser mode-locked by black phosphorus saturable absorber. *CLEO: Science and Innovations*. Optical Society of America, 2018.

[223] Y. Hu, X. Jin, G. Hu, et al., Eds. Hybrid mode-locked erbium-doped fiber laser with black phosphorus saturable absorber. *2018 Conference on Lasers and Electro-Optics (CLEO)*; 2018: IEEE.

[224] X. Jin, G. Hu, M. Zhang, et al., Eds. Long term stable black phosphorus saturable absorber for mode-locked fiber laser. *CLEO: Science and Innovations*. Optical Society of America, 2017.

[225] X. Jin, G. Hu, M. Zhang, et al., "102 fs pulse generation from a long-term stable, inkjet-printed black phosphorus-mode-locked fiber laser," *Optics Express*, vol. 26, pp. 12506–12513, 2018.

[226] C. Zhao, Y. Zou, Y. Chen, et al., "Wavelength-tunable picosecond soliton fiber laser with topological insulator: Bi_2Se_3 as a mode locker," *Optics Express*, vol. 20, pp. 27888–27895, 2012.

[227] H. Liu, X.-W. Zheng, M. Liu, et al., "Femtosecond pulse generation from a topological insulator mode-locked fiber laser," *Optics Express*, vol. 22, pp. 6868–6873, 2014.

[228] M. Liu, N. Zhao, H. Liu, et al., "Dual-wavelength harmonically mode-locked fiber laser with topological insulator saturable absorber," *IEEE Photon. Technol. Lett.*, vol. 26, pp. 983–986, 2014.

[229] L. Gao, T. Zhu, W. Huang, and Z. Luo, "Stable, ultrafast pulse mode-locked by topological insulator Bi_2Se_3 nanosheets interacting with photonic crystal fiber: from anomalous dispersion to normal dispersion," *IEEE Photon. J.*, vol. 7, pp. 1–8, 2015.

[230] K. Li, Y. Song, Z. Yu, and J. Tian, Eds. A 359fs Er-doped fiber laser based on topological insulator: Bi_2Se_3. *Conference on Lasers and Electro-Optics/Pacific Rim*. Optical Society of America, 2015.

[231] R. Miao, M. Tong, K. Yin, et al., "Soliton mode-locked fiber laser with high-quality MBE-grown Bi_2Se_3 film," *Chinese Opt. Lett.*, vol. 17, 2019, Art no. 071403.

[232] K. Li, Y. Song, Z. Yu, R. Xu, Z. Dou, and J. Tian, "L-band femtosecond fibre laser based on Bi_2Se_3 topological insulator," *Laser Phys. Lett.*, vol. 12, 2015, Art no. 105103.

[233] J. Lee, J. Koo, and J. H. Lee, "A pulse-width-tunable, mode-locked fiber laser based on dissipative soliton resonance using a bulk-structured Bi_2Te_3topological insulator," *Opt. Eng.*, vol. 55, 2016, Art no. 081309.

[234] Z.-C. Luo, M. Liu, H. Liu, et al., "2 GHz passively harmonic mode-locked fiber laser by a microfiber-based topological insulator saturable absorber," *Opt. Lett.*, vol. 38, pp. 5212–5215, 2013.

[235] J. Lee, J. Koo, Y. M. Jhon, and J. H. Lee, "A femtosecond pulse erbium fiber laser incorporating a saturable absorber based on bulk-structured Bi_2Te_3 topological insulator," *Optics Express*, vol. 22, pp. 6165–6173, 2014.

[236] J. Lee, J. Koo, C. Chi, and J. H. Lee, Eds. A harmonically mode-locked femtosecond fiber laser using bulk-structured Bi_2Te_3 topological insulator. *2015 Conference on Lasers and Electro-Optics (CLEO)*. IEEE, 2015.

[237] D. Mao, B. Jiang, X. Gan, et al., "Soliton fiber laser mode locked with two types of film-based Bi_2Te_3 saturable absorbers," *Photon. Res.*, vol. 3, pp. A43–A46, 2015.

[238] Q. Wei, K. Niu, X. Han, et al., "Large energy pulses generation in a mode-locked Er-doped fiber laser based on CVD-grown Bi_2Te_3 saturable absorber," *Opt. Mater. Express*, vol. 9, pp. 3535–3545, 2019.

[239] P. Yan, R. Lin, S. Ruan, et al., "A practical topological insulator saturable absorber for mode-locked fiber laser," *Sci. Rep.*, vol. 5, 2015, Art no. 8690.

[240] J. Lee, Y. Kim, K. Lee, and J. H. Lee, "Femtosecond mode-locking of a fiber laser using a $CoSb_3$-skutterudite-based saturable absorber," *Photon. Res.*, vol. 6, pp. C36–C43, 2018.

[241] H. Xia, H. Li, C. Lan, et al., Eds. Erbium-doped fiber laser mode-locked with a few-layer MoS_2 saturable absorber. *2014 Asia Communications and Photonics Conference (ACP)*. IEEE, 2014.

[242] T. H. Chen, C.-Y. Lin, Y.-H. Lin, et al., "MoS_2 nano-flake doped polyvinyl alcohol enabling polarized soliton mode-locking of fiber laser," *Int. J. Mater. Chem. C*, vol. 10, 2016, https://doi.org/10.1039/C6TC02623K.

[243] C. Liu, H. Li, G. Deng, C. Lan, C. Li, and Y. Liu, Eds. Femtosecond Er-doped fiber laser using a graphene/MoS_2 heterostructure saturable absorber. *2016 Asia Communications and Photonics Conference (ACP)*. IEEE, 2016.

[244] M. Ahmed, A. Latiff, H. Arof, and S. W. Harun, "Mode-locking pulse generation with MoS_2–PVA saturable absorber in both anomalous and ultra-long normal dispersion regimes," *Appl. Optic.*, vol. 55, pp. 4247–4252, 2016.

[245] D. Steinberg, J. D. Zapata, E. A. T. de Souza, and L. A. Saito, "Mechanically exfoliated graphite onto D-shaped optical fiber for femtosecond mode-locked Erbium-doped fiber laser," *J. Lightwave Technol.*, vol. 36, pp. 1868–1874, 2018.

[246] R. Khazaeizhad, S. H. Kassani, H. Jeong, D.-I. Yeom, and K. Oh, "Mode-locking of Er-doped fiber laser using a multilayer MoS_2 thin film as a saturable absorber in both anomalous and normal dispersion regimes," *Optics Express*, vol. 22, pp. 23732–23742, 2014.

[247] M. Liu, X.-W. Zheng, Y.-L. Qi, et al., "Microfiber-based few-layer MoS_2 saturable absorber for 2.5 GHz passively harmonic mode-locked fiber laser," *Optics Express*, vol. 22, pp. 22841–22846, 2014.

[248] F. Lu, X. Liu, and H. Yang, Eds. MoS_2-mode-locked fiber laser delivering ultrashort pulses with three types of sidebands. *Bragg Gratings, Photosensitivity, and Poling in Glass Waveguides*. Optical Society of America, 2016.

[249] Y. Wang, D. Mao, X. Gan, et al., "Harmonic mode locking of bound-state solitons fiber laser based on MoS_2 saturable absorber," *Optics Express*, vol. 23, pp. 205–210, 2015.

[250] E. J. Aiub, D. Steinberg, E. A. T. de Souza, and L. A. Saito, "200-fs mode-locked Erbium-doped fiber laser by using mechanically exfoliated MoS_2 saturable absorber onto D-shaped optical fiber," *Optics Express*, vol. 25, pp. 10546–10552, 2017.

[251] H. Liu, A.-P. Luo, F.-Z. Wang, et al., "Femtosecond pulse erbium-doped fiber laser by a few-layer MoS_2 saturable absorber," *Opt. Lett.*, vol. 39, pp. 4591–4594, 2014.

[252] K. Wu, X. Zhang, J. Wang, and J. Chen, "463-MHz fundamental mode-locked fiber laser based on few-layer MoS_2 saturable absorber," *Opt. Lett.*, vol. 40, pp. 1374–1377, 2015.

[253] H. Xia, H. Li, C. Lan, et al., "Ultrafast erbium-doped fiber laser mode-locked by a CVD-grown molybdenum disulfide (MoS_2) saturable absorber," *Optics Express*, vol. 22, pp. 17341–17348, 2014.

[254] W. Liu, M. Liu, B. Liu, et al., "Nonlinear optical properties of MoS_2-WS_2 heterostructure in fiber lasers," *Optics Express*, vol. 27, pp. 6689–6699, 2019.

[255] W. Liu, Y.-N. Zhu, M. Liu, et al., "Optical properties and applications for MoS_2-Sb_2Te_3-MoS_2 heterostructure materials," *Photon. Res.*, vol. 6, pp. 220–227, 2018.

[256] M. Liu, W. Liu, and Z. Wei, "$MoTe_2$ saturable absorber with high modulation depth for erbium-doped fiber laser," *J. Lightwave Technol.*, vol. 37, pp. 3100–31005, 2019.

[257] X. Han, "2D $MoTe_2$ film as a saturable absorber for a wavelength-tunable ultrafast fiber laser," *Appl. Optic.*, vol. 58, pp. 8390–8395, 2019.

[258] J. Wang, Z. Jiang, H. Chen, et al., "High energy soliton pulse generation by a magnetron-sputtering-deposition-grown $MoTe_2$ saturable absorber," *Photon. Res.*, vol. 6, pp. 535–541, 2018.

[259] J. Lee, K. Lee, S. Kwon, B. Shin, and J. H. Lee, "Investigation of nonlinear optical properties of rhenium diselenide and its application as a femtosecond mode-locker," *Photon. Res.*, vol. 7, pp. 984–993, 2019.

[260] X. Xu, M. He, C. Quan, et al., "Saturable absorption properties of ReS_2 films and mode-locking application based on double covered ReS_2 micro-fiber," *J. Lightwave Technol.*, vol. 1, 2018. https://doi.org/10.1109/JLT.2018.2870433.

[261] X. Zhu, S. Chen, M. Zhang, et al., "TiS_2-based saturable absorber for ultrafast fiber lasers," *Photon. Res.*, vol. 6, pp. C44–C48, 2018.

[262] W. Liu, L. Pang, H. Han, et al., "70-fs mode-locked erbium-doped fiber laser with topological insulator," *Sci. Rep.*, vol. 6, 2016, Art no. 19997.

[263] J. Bogusławski, G. Soboń, R. Zybała, et al., "Investigation on pulse shaping in fiber laser hybrid mode-locked by Sb_2Te_3 saturable absorber," *Optics Express*, vol. 23, pp. 29014–29023, 2015.

[264] J. Boguslawski, J. Sotor, G. Sobon, et al., "Mode-locked Er-doped fiber laser based on liquid phase exfoliated Sb_2Te_3 topological insulator," *Laser Phys.*, vol. 24, 2014, Art no. 105111.

[265] J. Boguslawski, G. Sobon, R. Zybala, and J. Sotor, "Dissipative soliton generation in Er-doped fiber laser mode-locked by Sb_2Te_3 topological insulator," *Opt. Lett.*, vol. 40, pp. 2786–2789, 2015.

[266] J. Boguslawski, J. Sotor, G. Sobon, et al., Eds. Sub-200 fs dissipative soliton Er-doped fiber laser mode-locked by Sb_2Te_3 topological insulator. *The European Conference on Lasers and Electro-Optics*. Optical Society of America, 2015.

[267] J. Sotor, G. Sobon, K. Krzempek, K. M. Abramski, Eds. Er-doped fiber laser mode-locked by mechanically exfoliated Sb_2Te_3 saturable absorber. *Nonlinear Optics*: Optical Society of America, 2013.

[268] J. Sotor, G. Sobon, and K. M. Abramski, "Sub-130 fs mode-locked Er-doped fiber laser based on topological insulator," *Optics Express*, vol. 22, pp. 13244–13249, 2014.

[269] J. Sotor, G. Sobon, W. Macherzynski, P. Paletko, K. Grodecki, and K. M. Abramski, "Mode-locking in Er-doped fiber laser based on mechanically exfoliated Sb_2Te_3 saturable absorber," *Opt. Mater. Express*, vol. 4, pp. 1–6, 2014.

[270] J. Sotor, G. Sobon, W. Macherzynski, and K. Abramski, "Harmonically mode-locked Er-doped fiber laser based on a Sb_2Te_3 topological insulator saturable absorber," *Laser Phys. Lett.*, vol. 11, 2014, Art no. 055102.

[271] R. Khazaeizhad, S. H. Kassani, H. Jeong, D.-I. Yeom, and K. Oh, editors. Passively mode-locked fiber laser based on CVD WS_2. *2015 Conference on Lasers and Electro-Optics (CLEO)*. IEEE, 2015.

[272] K. Wu, X. Zhang, J. Wang, X. Li, and J. Chen, "WS_2 as a saturable absorber for ultrafast photonic applications of mode-locked

and Q-switched lasers," *Optics Express*, vol. 23, pp. 11453–11461, 2015.
[273] B. Liu, X. Yang, Y. Luo, et al., "Soliton molecules in a fiber laser based on optic evanescent field interaction with WS_2," *Appl. Phys. B*, vol. 124, pp. 151, 2018.
[274] R. Khazaeinezhad, S. H. Kassani, H. Jeong, D.-I. Yeom, and K. Oh, "Femtosecond soliton pulse generation using evanescent field interaction through Tungsten disulfide (WS_2) film," *J. Lightwave Technol.*, vol. 33, pp. 3550–3557, 2015.
[275] D. Mao, S. Zhang, Y. Wang, et al., "WS_2 saturable absorber for dissipative soliton mode locking at 1.06 and 1.55 μm," *Optics Express*, vol. 23, pp. 27509–27519, 2015.
[276] P. Yan, A. Liu, Y. Chen, et al., "Microfiber-based WS_2-film saturable absorber for ultra-fast photonics," *Opt. Mater. Express*, vol. 5, pp. 479–489, 2015.
[277] P. Yan, A. Liu, Y. Chen, et al., "Passively mode-locked fiber laser by a cell-type WS_2 nanosheets saturable absorber," *Sci. Rep.*, vol. 5, 2015, Art no. 12587.
[278] J. Koo, Y. I. Jhon, J. Park, J. Lee, Y. M. Jhon, and J. H. Lee, "Near-Infrared saturable absorption of defective bulk-structured WTe_2 for femtosecond laser mode-locking," *Adv. Funct. Mater.*, vol. 26, pp. 7454–7461, 2016.
[279] X. Li, W. Xu, Z. Hui, P. Guo, J. Liu, and Y. Zhang, "Cu_2S nanosheets for ultrashort pulse generation in near-infrared regions," *Nanoscale*, vol. 11, pp. 6045–6051, 2019.
[280] Y. Li, X. Zhao, H. Zhang, and M. Li, "GaSe saturable absorber for mode-locked Er-doped fiber laser," *Infrared Phys. Technol.*, vol. 96, pp. 325–329, 2019.
[281] Z. Hui, W. Xu, X. Li, P. Guo, Y. Zhang, and J. Liu, "Cu_2S nanosheets for ultrashort pulse generation in the near-infrared region," *Nanoscale*, vol. 11, pp. 6045–6051, 2019.
[282] H. Ahmad, S. Soltani, K. Thambiratnam, M. Yasin, and Z. Tiu, "Mode-locking in Er-doped fiber laser with reduced graphene oxide on a side-polished fiber as saturable absorber," *Opt. Fiber Technol.*, vol. 50, pp. 177–182, 2019.
[283] W. A. Khaleel, S. A. Sadeq, I. Alani, and M. Ahmed, "Magnesium oxide (MgO) thin film as saturable absorber for passively mode locked erbium-doped fiber laser," *Optic Laser. Technol.*, vol. 115, pp. 331–336, 2019.
[284] Q. Wu, M. Zhang, X. Jin, et al., Eds. 104fs mode-locked fiber laser with a MXene-based saturable absorber. *CLEO: Applications and Technology*. Optical Society of America, 2019.
[285] J. Li, Z. Zhang, L. Du, et al., "Highly stable femtosecond pulse generation from a MXene $Ti_3C_2T_x$ (T= F, O, or OH) mode-locked fiber laser," *Photon. Res.*, vol. 7, pp. 260–264, 2019.
[286] C. Dou, W. Wen, J. Wang, et al., "Ternary $ReS_{2(1-x)}Se_{2x}$ alloy saturable absorber for passively Q-switched and mode-locked erbium-doped all-fiber lasers," *Photon. Res.*, vol. 7, pp. 283–288, 2019.
[287] K. Niu, R. Sun, Q. Chen, B. Man, and H. Zhang, "Passively mode-locked Er-doped fiber laser based on SnS_2 nanosheets as a saturable absorber," *Photon. Res.*, vol. 6, pp. 72–76, 2018.
[288] Y. I. Jhon, J. Lee, M. Seo, J. H. Lee, and Y. M. Jhon, "van der Waals layered tin selenide as highly nonlinear ultrafast saturable absorber," *Adv. Opt. Mater.*, vol. 7, 2019, Art no. 1801745.
[289] J. Wang, Z. Jiang, H. Chen, et al., "High energy soliton pulse generation by a magnetron-sputtering-deposition-grown $MoTe_2$ saturable absorber," *Photon. Res.*, vol. 6, 2018, https://doi.org/10.1364/prj.6.000535.
[290] M. Pawliszewska, A. Duzynska, M. Zdrojek, and J. Sotor, "Metallic carbon nanotube-based saturable absorbers for holmium-doped fiber lasers," *Optics Express*, vol. 27, pp. 11361–11369, 2019.
[291] H. Yu, X. Zheng, K. Yin, X. Cheng, and T. Jiang, "Thulium/holmium-doped fiber laser passively mode locked by black phosphorus nanoplatelets-based saturable absorber," *Appl. Optic.*, vol. 54, pp. 10290–10294, 2015.
[292] M. Pawliszewska, Y. Ge, Z. Li, H. Zhang, and J. Sotor, "Fundamental and harmonic mode-locking at 2.1 μm with black phosphorus saturable absorber," *Optics Express*, vol. 25, pp. 16916–16921, 2017.
[293] J. Sotor, G. Sobon, M. Kowalczyk, W. Macherzynski, P. Paletko, and K. M. Abramski, "Ultrafast thulium-doped fiber laser mode locked with black phosphorus," *Opt. Lett.*, vol. 40, pp. 3885–3888, 2015.
[294] M. A. Solodyankin, E. D. Obraztsova, A. S. Lobach, et al., "Mode-locked 1.93μm thulium fiber laser with a carbon nanotube absorber," *Opt. Lett.*, vol. 33, pp. 1336–1338, 2008.
[295] Y. Chen, J. Zhai, X. Xu, et al., "Mode-locked thulium-doped fiber laser based on 0.3 nm diameter single-walled carbon nanotubes at 1.95 μm," *Chinese Opt. Lett.*, vol. 15, pp. 41403–41406, 2017.
[296] K. Kieu and F. W. Wise, "Soliton thulium-doped fiber laser with carbon nanotube saturable absorber," *IEEE Photon. Technol. Lett.*, vol. 21, pp. 128–130, 2009.
[297] M. A. Chernysheva, A. A. Krylov, P. G. Kryukov, et al., "Thulium-doped mode-locked all-fiber laser based on NALM and carbon nanotube saturable absorber," *Optics Express*, vol. 20, pp. B124–B130, 2012.
[298] M. Zhang, E. J. R. Kelleher, F. Torrisi, et al., "Tm-doped fiber laser mode-locked by graphene-polymer composite," *Optics Express*, vol. 20, pp. 25077–25084, 2012.
[299] Q. Wang, T. Chen, B. Zhang, M. Li, Y. Lu, and K. P. Chen, "All-fiber passively mode-locked thulium-doped fiber ring laser using optically deposited graphene saturable absorbers," *Appl. Phys. Lett.*, vol. 102, 2013, https://doi.org/10.1063/1.4800036.
[300] G. Sobon, J. Sotor, I. Pasternak, A. Krajewska, W. Strupinski, and K. M. Abramski, "Thulium-doped all-fiber laser mode-locked by CVD-graphene/PMMA saturable absorber," *Optics Express*, vol. 21, pp. 12797–12802, 2013.
[301] G. Sobon, J. Sotor, I. Pasternak, A. Krajewska, W. Strupinski, and K. M. Abramski, "All-polarization maintaining, graphene-based femtosecond Tm-doped all-fiber laser," *Optics Express*, vol. 23, pp. 9339–9346, 2015.
[302] J. Sotor, J. Boguslawski, T. Martynkien, et al., "All-polarization-maintaining, stretched-pulse Tm-doped fiber laser, mode-locked by a graphene saturable absorber," *Opt. Lett.*, vol. 42, pp. 1592–1595, 2017.
[303] M. Jung, J. Koo, J. Park, et al., "Mode-locked pulse generation from an all-fiberized, Tm-Ho-codoped fiber laser incorporating a graphene oxide-deposited side-polished fiber," *Optics Express*, vol. 21, pp. 20062–20072, 2013.
[304] M. F. M. Rusdi, A. H. A. Rosol, M. F. A. Rahman, et al., "Q-switched and mode-locked thulium doped fiber lasers with nickel oxide film saturable absorber," *Optic Commun.*, vol. 447, pp. 6–12, 2019.

[305] K. Yin, B. Zhang, L. Li, T. Jiang, X. Zhou, and J. Hou, "Soliton mode-locked fiber laser based on topological insulator Bi_2Te_3 nanosheets at 2 μm," *Photon. Res.*, vol. 3, 2015.

[306] J. Lee, Y. Kim, and J. H. Lee, editors. Femtosecond Tm-Ho Co-Doped Fiber Laser using a CoSb3-Skutterudite-Based Passive Mode-Locker. *2019 Conference on Lasers and Electro-Optics Europe & European Quantum Electronics Conference (CLEO/Europe-EQEC)*: IEEE, 2019.

[307] Z. Tian, K. Wu, L. Kong, et al., "Mode-locked thulium fiber laser with MoS_2," *Laser Phys. Lett.*, vol. 12, 2015, https://doi.org/10.1088/1612-2011/12/6/065104.

[308] J. Lee, J. Koo, J. Lee, Y. M. Jhon, and J. H. Lee, "All-fiberized, femtosecond laser at 1912 nm using a bulk-like $MoSe_2$ saturable absorber," *Opt. Mater. Express*, vol. 7, 2017, https://doi.org/10.1364/ome.7.002968.

[309] M. Jung, J. Lee, J. Park, J. Koo, Y. M. Jhon, and J. H. Lee, "Mode-locked, 1.94-μm, all-fiberized laser using WS_2 based evanescent field interaction," *Optics Express*, vol. 23, pp. 19996–20006, 2015.

[310] Q. Jiang, M. Zhang, Q. Zhang, et al., Eds. Thulium-doped mode-locked fiber laser with MXene saturable absorber. *CLEO: Science and Innovations*. Optical Society of America; 2019.

[311] Y. Zhang, J. Wang, M. Ma, et al., "Mode-locked Tm-doped fiber laser with large modulation depth $ReS_{1.02}Se_{0.98}$ nanosheet saturable absorber," *Jpn. J. Appl. Phys.*, vol. 58, 2019, https://doi.org/10.7567/1347-4065/ab4003.

[312] W. Shi, Q. Fang, X. Zhu, R. A. Norwood, and N. Peyghambarian, "Fiber lasers and their applications," *Appl. Optic.*, vol. 53, pp. 6554–6568, 2014.

[313] J. Scherer, J. Paul, H. Jost, and M. L. Fischer, "Mid-IR difference frequency laser-based sensors for ambient CH_4, CO, and N_2O monitoring," *Appl. Phys. B*, vol. 110, pp. 271–277, 2013.

[314] C. Frerichs, and U. B. Unrau, "Passive Q-switching and mode-locking of erbium-doped fluoride fiber lasers at 2.7 μm," *Opt. Fiber Technol.*, vol. 2, pp. 358–366, 1996.

[315] Z. Qin, G. Xie, C. Zhao, S. Wen, P. Yuan, and L. Qian, "Mid-infrared mode-locked pulse generation with multilayer black phosphorus as saturable absorber," *Opt. Lett.*, vol. 41, pp. 56–59, 2016.

[316] K. Yin, T. Jiang, X. Zheng, H. Yu, X. Cheng, and J. Hou, Mid-infrared ultra-short mode-locked fiber laser utilizing topological insulator Bi_2Te_3 nano-sheets as the saturable absorber. *arXiv preprint arXiv*, 2015.

[317] Z. Qin, G. Xie, J. Ma, P. Yuan, and L. Qian, "28 μm all-fiber Q-switched and mode-locked lasers with black phosphorus, *Photon. Res.*, vol. 6, 2018, https://doi.org/10.1364/prj.6.001074.

[318] Z. Qin, T. Hai, G. Xie, et al., "Black phosphorus Q-switched and mode-locked mid-infrared Er:ZBLAN fiber laser at 3.5 mum wavelength," *Optics Express*, vol. 26, pp. 8224–8231, 2018.

[319] J. Li, H. Luo, B. Zhai, et al., "Black phosphorus: a two-dimension saturable absorption material for mid-infrared Q-switched and mode-locked fiber lasers," *Sci. Rep.*, vol. 6, 2016, Art no. 30361.

[320] G. Zhu, X. Zhu, F. Wang, et al., "Graphene mode-locked fiber laser at 2.8 μm," *IEEE Photon. Technol. Lett.*, vol. 28, pp. 7–10, 2016.